BJP British Journal of Pharmacology

DOI:10.1111/bph.12752
www.brjpharmacol.org

RESEARCH PAPER

Electromechanical and atrial and ventricular antiarrhythmic actions of CIJ-3-2F, a novel benzyl-furoquinoline vasodilator in rat heart

Gwo-Jyh Chang[1], Yung-Hsin Yeh[2], Tsung-Pin Lin[3], Chi-Jen Chang[2] and Wei-Jan Chen[2]

[1]*Graduate Institute of Clinical Medicinal Sciences, College of Medicine, Chang Gung University, Tao-Yuan, Taiwan,* [2]*First Cardiovascular Division of Medicine, Chang Gung Memorial Hospital, Tao-Yuan, Taiwan, and* [3]*Graduate Institute of Pharmaceutical Chemistry, China Medical University, Taichung, Taiwan*

Correspondence
Gwo-Jyh Chang, Graduate Institute of Clinical Medicinal Sciences, College of Medicine, Chang Gung University, 259 Wen-Hwa 1st Road, Kwei-Shan, Tao-Yuan 333, Taiwan. E-mail: gjchang@mail.cgu.edu.tw

Received
2 December 2013
Revised
27 March 2014
Accepted
21 April 2014

BACKGROUND AND PURPOSE
This study was designed to examine the antiarrhythmic efficacy and the underlying mechanisms of the benzyl-furoquinoline vasodilator, CIJ-3-2F, in rat cardiac preparations.

EXPERIMENTAL APPROACH
Conduction electrograms and left ventricular pressure were determined in Langendorff-perfused hearts. Action potentials were assessed with microelectrode techniques, calcium transients by fura-2 fluorescence and ionic currents by whole-cell patch-clamp techniques.

KEY RESULTS
In isolated hearts, CIJ-3-2F prolonged sinus cycle length, QT interval, Wenckebach cycle length, atrio-His bundle and His bundle-ventricular conduction intervals, refractory periods in atrium, AV node, His-Purkinje system and ventricle, and also increased left ventricular pressure. CIJ-3-2F reduced the incidences of both ischaemic and reperfusion-induced ventricular arrhythmias and prevented the induction of atrial tachyarrhythmias. In both atrial and papillary muscles, CIJ-3-2F decreased upstroke velocity and prolonged duration of the action potential. In ventricular myocytes, CIJ-3-2F moderately increased the amplitude of $[Ca^{2+}]_i$ transients and cell shortening. CIJ-3-2F inhibited the transient outward K^+ current (I_{to}) (IC_{50} = 4.4 μM) with accelerated inactivation, a slower rate of recovery from inactivation and use-dependency. CIJ-3-2F also suppressed the steady-state outward K^+ current (I_{ss}, IC_{50} = 3.6 μM, maximum inhibition = 65.7%) and both the inward Na^+ current (I_{Na}, IC_{50} = 2.8 μM) and L-type Ca^{2+} current ($I_{Ca,L}$, IC_{50} = 4.9 μM, maximum inhibition = 69.4%).

CONCLUSIONS AND IMPLICATIONS
CIJ-3-2F blocked Na^+ and I_{to} channels and, to some extent, also blocked Ca^{2+} and I_{ss} channels, modifying cardiac electromechanical function. These effects are likely to underlie its antiarrhythmic properties.

Abbreviations
AERP, atrial effective refractory period; APA, action potential amplitude; $APD_{25,\ 50,\ 90}$, action potential duration measured at 25, 50 and 90% repolarization; CIJ-3-2F, *N*-(2-fluoro-benzyl)-7-bromo-2,3,4,9-tetrahydrofuro[2,3-*b*]quinoline-3,4-dione; $I_{Ca,L}$, L-type Ca^{2+} inward current; I_{KI1}, inward rectifier K^+ current; I_{Na}, Na^+ inward current; I_{ss}, steady-state outward K^+ current; I_{to}, transient outward K^+ current; k, slope factor; RMP, resting membrane potential; SR, sarcoplasmic reticulum; VF, ventricular fibrillation; $V_{h,}$ half-maximal potential; V_{max}, maximum upstroke velocity of action potential; VPB, ventricular premature beats; VT, ventricular tachycardia; WCL, Wenckebach cycle length

Introduction

Atrial and ventricular tachyarrhythmias are believed to be one of the leading causes of death. In particular, life-threatening ventricular arrhythmias remains a serious problem in patients with coronary heart disease or myocardial infarction and most of these arrhythmias require treatment with antiarrhythmic drugs. As many patients with serious ventricular arrhythmias have reduced left ventricular ejection function (Schlepper, 1989), cardiac depression represents a serious adverse effect of class I antiarrhythmic agents. In contrast, drugs of the class III type may not impair the contractile function of the myocardium (Singh and Nademanee, 1985). The antiarrhythmic benefit afforded by class III agents is due to a prolongation of the action potential duration (APD) and refractoriness that causes the wavelength of activation to exceed the path length of the re-entrant circuit, thereby preventing initiation or maintenance of re-entrant excitation (Singh and Nademanee, 1985). Most selective class III agents, however, lose their effectiveness during tachycardia and may enhance the proarrhythmic potential during bradycardia (Hondeghem and Snyders, 1990) and these effects may reduce their therapeutic use (Waldo *et al.*, 1996). Therefore, attention has shifted to compounds with multiple effects on different ion channels. In support of the possible therapeutic benefit of such compounds, previous reports have shown that a balanced inhibition of K^+ and Ca^{2+} and/or Na^+ channels can result in a moderate prolongation of APD with a lesser proarrhythmic risk (Kodama *et al.*, 1997; Bril *et al.*, 1998; Faivre *et al.*, 1999; Amos *et al.*, 2001; Takács *et al.*, 2003; Lacerda *et al.*, 2010) although with some exceptions, such as bepridil (Singh, 1992).

Acrophyllidine, a furoquinoline alkaloid isolated from the plant *Acronychia halophylla*, has been reported to be a multichannel blocker in cardiomyocytes with proven effectiveness on ventricular tachyarrhythmias in rat hearts (Chang *et al.*, 2000). Our previous study also showed that acrophyllidine predominantly influenced electrophysiological properties in sinus nodal, atrioventricular (AV) nodal and ventricular tissues but had little effect on atrial tissue in the perfused rat heart (Chang *et al.*, 2000). In search of compounds derived from this alkaloid skeleton that had better cardiovascular actions, we investigated a series of analogues designed not only to extend acrophyllidine's antiarrhythmic activity but also to have additional vasorelaxant action. Among these analogues, *N*-(2-fluoro-benzyl)-7-bromo-2,3,4,9-tetrahydrofuro[2,3-*b*]quinoline-3,4-dione (CIJ-3-2F) is a newly synthesized halogen-containing benzyl-furoquinoline derivative in which the methoxyl group on the furoquinoline nucleus is substituted by a bromine atom (Chang *et al.*, 2010). This compound exhibited novel vasorelaxant, antiarrhythmic and inotropic activities. The mechanisms of action of CIJ-3-2F-induced vasorelaxation have been recently analysed and may include endothelium-dependent and -independent pathways (Chang *et al.*, 2010). In the present study, we have characterized the antiarrhythmic efficacy and detailed electromechanical actions of CIJ-3-2F in rat cardiac preparations. We have defined its effects on the conduction system and left ventricular pressure of isolated Langendorff-perfused rat hearts, as well as its effects on Ca^{2+} transients, cell shortening and ionic currents of cardiac myocytes.

Methods

All animal care and experimental procedures complied with the Guide for the Care and Use of Laboratory Animals published by the US National Institutes of Health (NIH publication No. 85-23, revised 1996) and was approved by our institutional review board. All studies involving animals are reported in accordance with the ARRIVE guidelines for reporting experiments involving animals (Kilkenny *et al.*, 2010; McGrath *et al.*, 2010). A total of 235 animals were used in the experiments described here.

For this study, adult male Sprague Dawley rats weighing 250–300 g (purchased from the National Laboratory Animal Center, Taipei) were anaesthetized with sodium pentobarbital (50 mg·kg^{-1}, i.p.) and given heparin (300 units·kg^{-1}, i.p.) and then killed by cervical dislocation. For the study of ischaemic and reperfusion-induced arrhythmias, adult non-pregnant female rats weighing 250–300 g were also used.

Intracardiac electrocardiogram recording experiments

Rat hearts were mounted on a Langendorff perfusion apparatus and perfused with oxygenated normal Tyrode solution at 37°C as described previously (Chang *et al.*, 2002; details in Supporting Information). Atrial pacing was used to determine intracardiac conduction parameters, Wenckebach cycle length (WCL) and effective refractory periods (ERP) of the atria, AV node and His-Purkinje system and the ventricular extrastimulation protocol was used to record ventricular ERP.

Antiarrhythmic testing

Ischaemia- and reperfusion-induced ventricular arrhythmias. Rat isolated hearts were perfused via the aorta with oxygenated low K^+ (3 mM) Tyrode solution at a constant pressure of 70 mmHg. The ECG was recorded with an ECGA amplifier (Hugo Sachs Electronik-Harvard Apparatus GmbH, March-Hugstetten, Germany) via two contact electrodes placed respectively on base and apex of the heart. Hearts were allowed to equilibrate for 20 min, then solution was switched in a blinded, randomized fashion to one of the three test solutions: vehicle control (DMSO 0.03%), 3 or 30 μM CIJ-3-2F. After a further 5 min perfusion, the left anterior descending coronary artery was ligated for 30 min, followed by 5 min of reperfusion as described by Tsuchihashi and Curtis (1991). A successful occlusion was shown by a 40–50% reduction in coronary flow, compared with pre-ischaemic values, and confirmed with approximately 40% mean occluded zone size (see below for method). Coronary flow was measured by an ultrasonic flowmeter (Model TS410, Transonic Systems Inc., Ithaca, NY, USA). The size of the occluded zone was quantified using disulphine blue dye (VN 150, EMD Millipore Co., Billerica, MA, USA) as described by Curtis and Hearse (1989a). Arrhythmias were defined according to the Lambeth Conventions (Walker *et al.*, 1988; Curtis *et al.*, 2013). Ventricular premature beats (VPB) were defined as discrete and identifiable premature QRS complexes; bigeminy as a rhythm in which a normal sinus beat is followed by a VPB, followed by another

normal beat, and so on; a run of two or three consecutive VPBs was defined as a salvo and a run of four or more as ventricular tachycardia (VT). Ventricular fibrillation (VF) was defined as a signal from which individual QRS deflections vary in amplitude and coupling interval on a cycle-to-cycle basis. Total VF was classified as reversible and sustained VF (SVF). SVF was defined as VF lasting continuously for more than 120 s. Any heart not in sinus rhythm during the 2 s before reperfusion was excluded from the reperfusion group. Further details in Supporting Information.

Electrically induced atrial arrhythmias. Atrial pacing was performed from the right atrial appendage using a pacing electrode. Atrial tachyarrhythmia was induced with burst pacing at 200 ms pacing cycle length and 10× diastolic threshold after every eighth basic paced beat (S_1). The burst pacing current consisted of a train of 100 square wave pulses (pulse duration: 1 ms), at a frequency of 100 Hz for a duration of 1 s. Drug was included in perfusion solution for 20 min after the control pacing protocol was completed. Further details in Supporting Information.

Electromechanical measurements on papillary muscles

The left atrial strip or left ventricular papillary muscle was mounted in a tissue bath and superfused at a rate of 20 mL·min^{-1} with oxygenated normal Tyrode solution. The preparation was then stimulated with 1.5 times-threshold strength pulses (pulse duration: 1 ms) at 1 Hz. Transmembrane potentials were recorded using conventional microelectrode techniques (Chang *et al.*, 2002). The mechanical response was recorded simultaneously by a bridge amplifier. Further details in Supporting Information.

Measurements of intracellular Ca^{2+} transients and cell shortening

Single rat ventricular myocytes were isolated as described previously (Chang *et al.*, 2002). The Ca^{2+} transients were monitored with the use of the fluorescence calcium indicator fura-2, as described previously (Chang *et al.*, 2013). During measurements, the cells were field-stimulated by 2 ms pulses at 1 Hz (~30–40% above the threshold). The ratio of the fluorescence at 340 nm excitation to that at 380 nm was used as an indicator of free $[Ca^{2+}]_i$. Cell shortening was measured with a video edge-detection system simultaneously with fluorescence signal measurement. Further details in Supporting Information.

Whole-cell patch-clamp recording

Ionic currents were recorded in whole-cell configuration at room temperature (25–27°C) as described previously (Chang *et al.*, 2002). After preparing the whole-cell recording configuration, a capacitive transient induced by a 10 mV step from a holding voltage of 0 mV was recorded and used for the calculation of cell capacitance. The average cell capacitance was 190.3 ± 6.6 pF (n = 35) in ventricular myocytes and 102.5 ± 4.7 pF (n = 21) in atrial myocytes. Command pulse generation, data acquisition and data analysis were performed on an IBM-compatible computer running pCLAMP 8.0 software using a 16-bit Digidata 1320A interface (Molecular Devices, Sunnyvale, CA, USA). Further details in Supporting Information.

Data analysis

With the exception of incidences of arrhythmias, all the results are expressed as the mean ± SEM. Within-group comparisons among control and post-treatment dosage parameters were made using an analysis of variance (ANOVA) for repeated measures with Dunnett's t test for multiple comparisons. Incidences of arrhythmias were compared by a $\chi 2$ procedure followed by pairwise comparison (Fisher's exact test). P-values of less than 0.05 were considered to indicate significant differences. Concentration-response curves were fitted by the following equation, $E = E_{max}/[1+(IC_{50}/C)^{nH}]$, where E is the effect at concentration C, E_{max} is maximal effect, IC_{50} is the concentration for half-maximal block and n_H is the Hill coefficient. Conductance of voltage-activated ion channel (G) was calculated according to the equation as follows: $G = I/(V_m - V_{rev})$, where I is the ionic current, V_{rev} is the reversal potential of this current, and V_m is the membrane potential. G_{max} is the maximal ionic conductance. The normalized G was plotted as a function of V_m (activation curve) and analyzed by using the Boltzmann equation as follows: $G/G_{max} = 1/\{1+\exp[(V_h - V_m)/k]\}$, Where V_h and k represent the voltage of activation midpoint and a slope factor, respectively. The inactivation curves of ionic current were fitted by the Boltzmann equation: $I/I_{max} = 1/\{1+\exp[(V_m - V_h)/k]\}$, where I gives the current amplitude and I_{max} its maximum, V_m the potential of prepulse, V_h the half-maximal inactivation potential, and k the slope factor. Sigmaplot 12.0 (Systat Software, Inc., Chicago, IL, USA) was used for fitting data with Boltzmann or other user-defined functions.

Solutions and drugs

The normal Tyrode solution contained (in mM): NaCl 137.0, KCl 5.4, $MgCl_2$ 1.1, $NaHCO_3$ 11.9, NaH_2PO_4 0.33, $CaCl_2$ 1.8 and dextrose 11.0. The low K^+ Tyrode solution contained (in mM): NaCl 118.5, KCl 3.0, $MgSO_4$ 1.2, $NaHCO_3$ 25.0, NaH_2PO_4 1.2, $CaCl_2$ 1.4 and dextrose 11.1. The HEPES-buffered Tyrode solution contained (in mM): NaCl 137.0, KCl 5.4, KH_2PO_4 1.2, $MgSO_4$ 1.22, $CaCl_2$ 1.8, dextrose 11.0, and HEPES 6.0, titrated to pH 7.4 with NaOH. The internal pipette filling solution contained (in mM): KCl 120.0, NaCl 10.0, MgATP 5.0, EGTA 5.0, and HEPES 10.0, adjusted to pH 7.2 with KOH. The Cs^+-containing pipette solution contained (in mM): CsCl 130.0, EGTA 5.0, tetraethylammonium (TEA) chloride 15.0, dextrose 5.0 and HEPES 10.0, adjusted to pH 7.2 with CsOH. CIJ-3-2F was synthesized by one of the authors, Dr. T. P. Lin. Its purity (> 99%) was confirmed by spectral methods (mass and NMR). Fura-2/AM and Pluronic F-127 were purchased from Molecular Probes (Eugene, Ore., USA); all other chemicals were purchased from Sigma-Aldrich Chem. Co. (St. Louis, MO, USA). CIJ-3-2F, Fura-2 AM, ryanodine, and thapsigargin were dissolved in DMSO. Other drugs were dissolved in physiological saline before the start of the experiment. In control experiments, DMSO (up to 0.1% v·v^{-1}) alone produced no significant effect on mechanical and electrophysiological variables of the heart preparations. CIJ-3-2F was prepared as a stock solution of the highest concentration of 100 mM in 100% DMSO. This stock solution was then used for most studies in multicellular preparations and when it was given in a cumulative manner to obtain each final concentration from 10 to 100 μM, the total amount of DMSO approximated to 0.1% v·v^{-1}. For the studies in single

cardiomyocytes, final concentrations (0.3, 1, 3, 10, 30 and 50 μM) of CIJ-3-2F were obtained by cumulative adding aliquots of corresponding stock solutions (2, 5, 20, 50, 100, and 100 mM) to the external solutions to limit the final concentration of DMSO to approximately 0.093% v·v^{-1}. During the experiments of ischaemic and reperfusion-induced arrhythmias, whatever the final concentrations of CIJ-3-2F, DMSO concentration was always equal to 0.03% v·v^{-1} in vehicle and drug solutions.

Results

Effects on the electrophysiological properties of the cardiac conduction system

In Langendorff-perfused rat hearts, CIJ-3-2F (≥10 μM) prolonged the basic cycle length, QT interval, WCL and the refractory periods of the atrium (AERP), AV node and His-Purkinje system in a concentration-dependent manner (Figure 1, Table 1). At higher concentrations (30 μM), the conduction intervals through the AV node (atrio-His bundle conduction interval) and the His-Purkinje system (His-ventricular conduction interval) and the refractory period of ventricle (ventricular effective refractory period) were also prolonged. CIJ-3-2F had almost no effect on the conduction interval through the atrial tissue (sinoatrial conduction interval), even at 30 μM. The effect of CIJ-3-2F on conduction parameters were reversible after perfusion with drug-free solution for 60 min. Application of the corresponding concentrations of vehicle (DMSO) produced no significant changes in the conduction parameters (Table 1).

Effects on ischaemia- and reperfusion-induced ventricular arrhythmias

Typical ECG changes recorded during ischaemia in a rat heart are shown in Figure 2A. In hearts from male rats, CIJ-3-2F reduced the incidence of ischaemia-induced arrhythmias in a concentration-dependent manner. At 3 μM, total VF and SVF were abolished (Table 2). At the highest concentration (30 μM), the incidences of VPB, bigeminy, salvo and VT were significantly reduced and total VF and SVF were abolished. CIJ-3-2F did not delay the onset of ischaemia-induced arrhythmias (Table 2). CIJ-3-2F was also effective on reperfusion-induced arrhythmias (Table 2). At 30 μM, CIJ-3-2F significantly delayed the onset of reperfusion-induced arrhythmias (Table 2) and increased coronary flow before, during and after ischaemia (Table 3). CIJ-3-2F had no effect on occluded zone size (Figure 2B, Table 3).

As clinical findings suggest that female gender is an independent factor for torsade de pointes arrhythmias (James

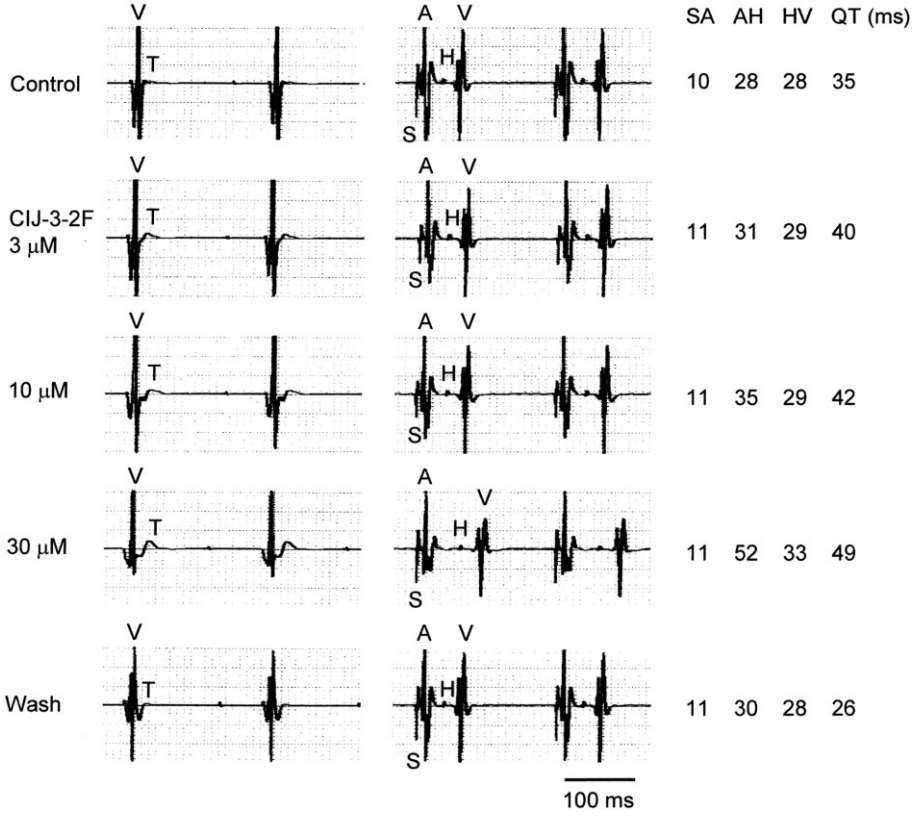

Figure 1

Effects of CIJ-3-2F on His bundle (right panel) and ventricular (left panel) electrograms recorded in an isolated, Langendorff-perfused, rat heart. The preparation was paced at a basic cycle length of 200 ms. A, atrial activity; H, His potential; S, stimulation artifact; T, ventricular repolarization; V, ventricular activity.

Table 1

Concentration-related effects of time-vehicle (DMSO) control and CIJ-3-2F on the conduction system of rat isolated perfused hearts

	BCL	SA	AH	HV	QT	WCL	AERP	AVNERP	HPFRP	VERP
Control	232 ± 8	9 ± 0	26 ± 1	19 ± 1	31 ± 3	112 ± 4	38 ± 3	82 ± 2	115 ± 4	30 ± 2
DMSO 0.003%	234 ± 10	10 ± 0	28 ± 1	19 ± 1	30 ± 2	114 ± 4	34 ± 2	84 ± 2	113 ± 3	31 ± 2
0.01%	234 ± 12	10 ± 0	28 ± 2	19 ± 1	29 ± 2	116 ± 5	37 ± 2	87 ± 3	114 ± 2	32 ± 3
0.03%	237 ± 13	10 ± 0	29 ± 2	20 ± 1	28 ± 2	117 ± 4	38 ± 2	87 ± 3	117 ± 3	32 ± 3
Washout	237 ± 13	10 ± 0	32 ± 1	20 ± 1	28 ± 2	126 ± 6	40 ± 2	98 ± 4	124 ± 5	37 ± 3
Control	254 ± 9	10 ± 0	34 ± 2	19 ± 1	34 ± 2	133 ± 5	35 ± 3	98 ± 3	137 ± 4	33 ± 3
CIJ-3-2F 3 μM	270 ± 9	10 ± 0	38 ± 2	20 ± 1	38 ± 2	144 ± 5	51 ± 6	114 ± 7	152 ± 6	33 ± 3
10 μM	299 ± 10*	11 ± 1	44 ± 2	21 ± 1	51 ± 4**	168 ± 7*	57 ± 5*	142 ± 7**	179 ± 6**	47 ± 5
30 μM	377 ± 18*	11 ± 1	57 ± 5**	24 ± 1**	62 ± 6**	212 ± 9#	79 ± 9#	183 ± 10#	218 ± 9#	66 ± 6**
Washout	310 ± 21	11 ± 1	45 ± 6	21 ± 1	39 ± 2	155 ± 13	47 ± 5	123 ± 15	157 ± 13	40 ± 4

Data (in ms) were obtained from nine (DMSO group) and 12 (CIJ-3-2F group) experiments and are expressed as mean ± SEM. SA, AH, HV and QT intervals were obtained at a pacing cycle length of 200 ms. In the present experimental protocol, the AV node usually became refractory to premature extrastimulation before the His-Purkinje system became refractory. Therefore, only the functional refractory period of the His-Purkinje system (HPFRP, the shortest conducted V_1V_2 interval) was measured. *$P < 0.05$, **$P < 0.01$, #$P < 0.001$; significantly different from control. AERP, atrial effective refractory period; AH, atrio-His bundle conduction interval; AVNERP, AV nodal effective refractory period; BCL, basic cycle length; HPFRP, His-Purkinje system functional refractory period; HV, His-ventricular conduction interval; QT, ventricular repolarization time (VT interval); SA, sinoatrial conduction interval; VERP, ventricular effective refractory period; WCL, Wenckebach cycle length.

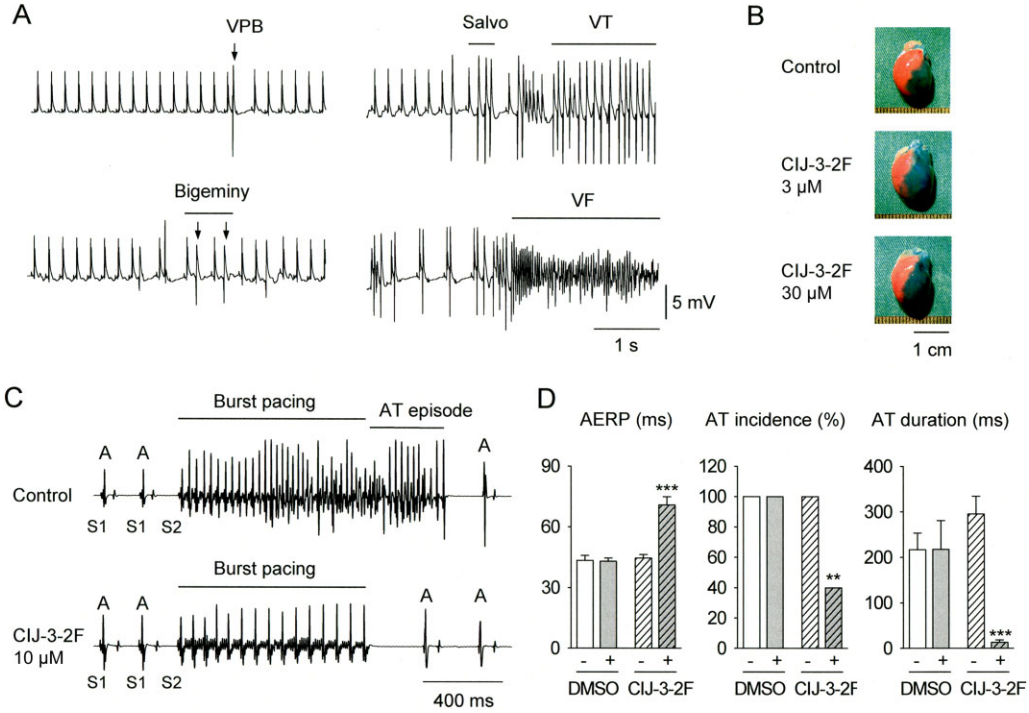

Figure 2

(A) Characteristic ECG of a male rat heart pretreated with vehicle (0.03% v·v^{-1} DMSO) during 30 min regional ischaemia. VPB, ventricular premature beats; VT, ventricular tachycardia; VF, ventricular fibrillation. (B) Representative male rat hearts from control- and drug-treated group showing occluded zone determined by disulphine blue dye exclusion method. (C) Recording of a typical atrial tachyarrhythmia (AT) episode elicited by burst pacing from an isolated heart at baseline (upper panel). AT was no longer induced 20 min after administration of CIJ-3-2F (10 μM) in the same heart (lower panel). (D) AERP was prolonged and both the incidence and duration of AT were significantly reduced by administration of CIJ-3-2F (10 μM, $n = 10$) but not by vehicle alone (0.01% v·v^{-1} DMSO, $n = 10$). **$P < 0.01$, ***$P < 0.001$; significantly different from baseline.

Table 2

The incidences and the time to onset of ischaemic or reperfusion-induced ventricular arrhythmias (Arr)

	Ischaemia									Reperfusion							
		Incidence (%)						Onset time of 1st Arr (log_{10} s)			Incidence (%)						Onset time of 1st Arr (log_{10} s)	
	n	VPB	BG	Salvo	VT	VF	SVF	*n*		*n*	VPB	BG	Salvo	VT	VF	SVF	*n*	
Male																		
DMSO 0.03%	12	100	92	92	100	75	33	12	2.53 ± 0.11	5	100	80	80	100	100	60	5	0.94 ± 0.24
CIJ-3-2F 3 μM	12	100	83	75	83	0#	0*	12	2.71 ± 0.12	12	100	75	58	100	67	0*	12	1.33 ± 0.07
30 μM	12	50**	33**	25**	25#	0#	0*	6	2.93 ± 0.08	12	67	17*	50	25**	8**	0*	9	1.94 ± 0.21*
Female																		
DMSO 0.03%	10	100	100	100	90	30	10	10	2.38 ± 0.23	7	100	71	86	100	71	43	7	1.08 ± 0.09
CIJ-3-2F 3 μM	10	90	90	90	90	20	10	9	2.52 ± 0.15	9	100	89	89	89	67	0	9	1.11 ± 0.18
30 μM	9	56*	22**	22**	22**	0	0	5	3.14 ± 0.09	8	38*	25	38	25**	0**	0	5	1.51 ± 0.06**

The incidence (as %) of ventricular premature beats (VPB), bigeminy (BG), salvos, ventricular tachycardia (VT), total ventricular fibrillation (VF) and sustained VF (SVF) are shown. Reperfusion-induced arrhythmias were quantified for 5 min of reperfusion. It should be noted that the size in some groups were reduced when assessing the reperfusion-induced arrhythmias because the remaining hearts were not in sinus rhythm at the moment of reperfusion and were thus excluded from analysis. Data of the onset time of the first arrhythmia (in log_{10} s) are expressed as mean ± SEM. Only those hearts having the arrhythmia during 30 min of ischaemia or 5 min of reperfusion were used for the calculations of onset time of arrhythmia. *$P < 0.05$, **$P < 0.01$, #$P < 0.001$; significantly different from the time-matched vehicle (DMSO) control group.

Table 3

Coronary flow and occluded zone size in hearts subjected to 30 min of ischaemia

		Coronary flow				
	n	1 min before drug	1 min before occlusion	1 min after occlusion	1 min after reperfusion	Occluded zone size (%)
Male						
DMSO 0.03%	12	11.7 ± 0.7	11.9 ± 0.8	5.8 ± 0.6	11.8 ± 0.7	39.4 ± 1.0
CIJ-3-2F 3 μM	12	11.4 ± 0.7	12.0 ± 0.8	5.0 ± 0.3	13.8 ± 0.7	39.7 ± 1.9
30 μM	12	11.4 ± 0.6	16.8 ± 1.0**	9.7 ± 0.6#	14.9 ± 0.7**	42.1 ± 1.1
Female						
DMSO 0.03%	10	13.2 ± 0.8	12.4 ± 0.9	5.0 ± 0.7	17.5 ± 0.7	43.1 ± 1.3
CIJ-3-2F 3 μM	10	10.9 ± 0.8	13.4 ± 0.8	6.2 ± 0.6	18.2 ± 1.7	45.2 ± 1.0
30 μM	9	11.4 ± 0.8	17.2 ± 1.0**	8.1 ± 0.4**	18.9 ± 1.0	44.9 ± 1.2

Values are expressed as mean ± SEM. Values of coronary flow before occlusion and after reperfusion were calculated from the total coronary flow and the weight of the ventricles and are expressed as $mL \cdot min^{-1} g^{-1}$. Values of coronary flow 1 min after occlusion are expressed as $mL \cdot min^{-1}$. The occluded zone size was quantified by the disulphine blue dye exclusion method and as a percentage of the total ventricular weight. $^{**}P < 0.01$, $^{\#}P < 0.001$; significantly different from the time-matched vehicle (DMSO) control group.

et al., 2007) and some findings observed that females had higher incidence of drug-induced torsade de pointes (Makkar *et al.*, 1993; Waldo *et al.*, 1996), we next investigated the effect of CIJ-3-2F in female hearts. As the incidence of ischaemia-induced total VF and SVF during perfusion with vehicle was very low (Table 2), it was not possible to examine the effects of CIJ-3-2F against ischaemia-induced total VF and SVF in female hearts. At 3 μM, CIJ-3-2F had no effects on ischaemia- and reperfusion-induced arrhythmias except that it abolished the occurrence of reperfusion-induced SVF (Table 2). At 30 μM, CIJ-3-2F significantly reduced the incidences of ischaemia- and reperfusion-induced arrhythmias and abolished the incidence of total VF and SVF. During perfusion with 3 or 30 μM CIJ-3-2F, no significant proarrhythmic effect was observed in these preparations. As in male rat hearts, CIJ-3-2F delayed the onset of reperfusion-induced arrhythmias and increased coronary flow but had no effect on occluded zone size in female hearts (Table 2 and 3).

Effects on electrically induced atrial arrhythmias

Representative recordings of electrically induced atrial tachyarrhythmias (AT) are shown in Figure 2C, and mean values for left atrial ERP and AT inducibility parameters are shown in Figure 2D. AT was easily induced by burst pacing at baseline (predrug) but not after 20 min of CIJ-3-2F (10 μM) administration (Figure 2C). CIJ-3-2F (10 μM) produced significant prolongation of the AERP and reductions in both the incidence and duration of AT (Figure 2D) in comparison with the DMSO vehicle (0.01%).

Effects on haemodynamic function in isolated hearts

For the recording procedure and the acute effects of CIJ-3-2F on haemodynamic function in isolated hearts, please see the Supporting Information (Supporting Information Figures S1 and S2).

Effects of CIJ-3-2F on action potential and contraction in papillary muscles and atrial strips

Concentration-dependent effects of CIJ-3-2F (10–100 μM) on action potential and contractile force in rat papillary muscles are illustrated in Figure 3A and Table 4. CIJ-3-2F prolonged the APD at 25, 50 and 90% repolarization in a concentration-dependent manner without affecting the resting membrane potential (RMP) or the action potential amplitude (APA). Higher concentration of CIJ-3-2F (100 μM) moderately decreased the maximum upstroke velocity of depolarization (V_{max}) and increased contractile force. The effects of CIJ-3-2F were partly reversed after a 50 min washout period. When the muscles received DMSO alone, electromechanical parameters remained unchanged throughout the study period (Supporting Information Table S1). Quinidine (75 μM), a well-studied class I_A agent, increased APD_{25}, APD_{50} and APD_{90}, while decreasing APA, V_{max} and contractile force, and having no significant effect on RMP (Figure 3B and Table 4). The prolongation of APD and increase in contractile force by CIJ-3-2F were also observed in the left atrial strips. However, CIJ-3-2F caused a significant decrease in APA and a much greater decrease in V_{max} in left atrial strips than in papillary muscles (Figure 3C and Table 4).

Effects of CIJ-3-2F on intracellular Ca^{2+} transients and cell shortening of ventricular myocytes

Representative traces depicting the acute actions of CIJ-3-2F (0.3–3 μM) on $[Ca^{2+}]_i$ transients and cell shortening are shown in Figure 4A. CIJ-3-2F in a concentration-dependent manner increased the amplitude of $[Ca^{2+}]_i$ transients with no significant alteration in the end-diastolic Ca^{2+} level, or the rising time or decay time constant (Figure 4A and B). Consistent with its effect on $[Ca^{2+}]_i$ transients, CIJ-3-2F increased the percent cell shortening with no significant effects on diastolic cell length or the kinetic parameters (Figure 4A and C).

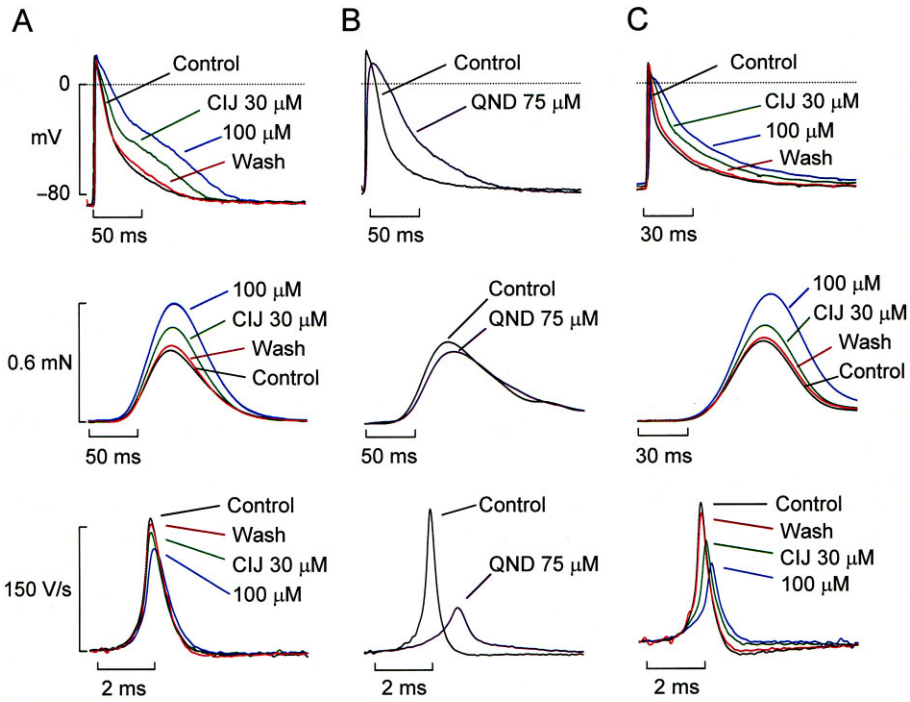

Figure 3

Superimposed tracings of transmembrane action potential, force of contraction and maximum upstroke velocity of action potential (V_{max}) from rat papillary muscles exposed to CIJ-3-2F (30 and 100 μM) (A) and quinidine (QND; 75 μM) (B) and a rat left atrial strip exposed to CIJ-3-2F (30 and 100 μM) (C). Stimulation frequency was 1 Hz. Each concentration of CIJ-3-2F was superfused in a cumulative manner. Upper traces are transmembrane action potentials; middle traces, contractile force; lower traces, V_{max}. Dashed lines represent zero potential level. All records were obtained after 20 min of exposure to each treatment. The washout records were obtained after superfusion with control solution for 60 min.

Application of the corresponding concentrations of vehicle (DMSO) produced no changes in any of these parameters (Supporting Information Figure S3). We measured sarcoplasmic reticulum (SR) Ca^{2+} content by emptying the SR with a rapid application of caffeine (10 mM). CIJ-3-2F (1 μM) increased the caffeine-induced $[Ca^{2+}]_i$ transient with no significant change in its decay time constant (Figure 5A and B). For comparison, the effects of 4-AP, a typical transient outward K^+ current (I_{to}) channel blocker, were examined in myocytes treated with 1 μM verapamil. Incubation with 4-AP (2 mM) increased the amplitude of $[Ca^{2+}]_i$ transients from 0.37 ± 0.02 to 0.46 ± 0.03 ($P < 0.05$, $n = 9$) and increased caffeine-induced $[Ca^{2+}]_i$ transients from 0.36 ± 0.01 to 0.45 ± 0.03 ($P < 0.05$, $n = 9$). To investigate the potential source(s) of the increase in $[Ca^{2+}]_i$ transients and SR Ca^{2+} content, we next tested whether the mechanism involved increasing Ca^{2+} handling in SR. The application of SR blockers 0.5 μM ryanodine (to deplete SR Ca^{2+} store and block Ca^{2+} release) or 0.5 μM thapsigargin (to block SR Ca^{2+} uptake) (Negretti *et al.*, 1993) decreased $[Ca^{2+}]_i$ transient amplitude (Figure 5C and D) while increased the diastolic $[Ca^{2+}]_i$ level (not shown). Figure 5C and D show that CIJ-3-2F still could increase both the amplitude of $[Ca^{2+}]_i$ transients and cell shortening and tended to increase SR Ca^{2+} content in myocytes pretreated with either ryanodine or thapsigargin, raising the possibility that the increased influx of Ca^{2+}, rather than SR-dependent mechanisms, were involved in these actions of CIJ-3-2F.

Effects of CIJ-3-2F on K^+ currents

Figure 6A shows the representative current traces recorded in response to depolarizing and hyperpolarizing steps to test potentials between +60 and −140 mV from a holding potential of −80 mV in a ventricular myocyte. CIJ-3-2F moderately reduced the amplitude of peak I_{to} but significantly accelerated its inactivation time course; the sustained current (I_{ss}) was simultaneously reduced by CIJ-3-2F. However, inward current through the inward rectifier K^+ channel (I_{K1}) was not significantly changed. Figure 6B and C illustrate the current density-voltage (*I–V*) relationships of peak K^+ currents (I_{to} and I_{K1}) and I_{ss} respectively. The inhibition of the I_{to} integral by 3 μM CIJ-3-2F was not voltage-dependent (Figure 6D). Figure 6E shows superimposed current traces elicited at +60 mV before and after cumulative application with 1, 3 and 10 μM CIJ-3-2F. As shown in Figure 6F 4-AP reduced the peak current amplitude without affecting the decay of I_{to} and the amplitude of $I_{ss,}$ as previously reported by Castle and Slawsky (1993) and Jahnel *et al.* (1994). The concentration-response curves derived for the inhibition of I_{to} and I_{ss} by CIJ-3-2F are shown in Figure 6G. The IC_{50} of CIJ-3-2F for inhibiting the I_{to} integral was 4.4 ± 1.0 μM, with an average E_{max} of 102.2 ± 7.6% (n_H = 1.18 ± 0.13, $n = 9$), and for inhibiting I_{ss} was 3.6 ± 1.5 μM, with an E_{max} of 65.7 ± 5.7 % (n_H = 1.12 ± 0.17, $n = 9$). Inhibition of I_{to} and I_{ss} by CIJ-3-2F was also observed in rat atrial myocytes (Supporting Information Figure S4A).

Table 4

Effects of increasing concentrations of CIJ-3-2F on action potentials and contractile forces recorded from rat ventricular papillary muscles and left atrial strips at a stimulation frequency of 1 Hz

	RMP (–mV)	APA (mV)	V_{max} (V·s^{-1})	APD_{25} (ms)	APD_{50} (ms)	APD_{90} (ms)	CF (%)
Papillary muscle (n = 11)							
Control	82.7 ± 0.9	103.5 ± 1.0	174.7 ± 6.7	7.3 ± 0.4	14.2 ± 0.6	55.5 ± 3.3	100.0 ± 0.0
CIJ-3-2F 10 μM	83.2 ± 1.1	104.8 ± 1.1	173.1 ± 7.4	7.6 ± 0.5	15.4 ± 0.8	61.0 ± 3.9	102.3 ± 2.6
30 μM	81.3 ± 1.4	103.9 ± 1.4	164.5 ± 6.8	11.3 ± 1.6	23.6 ± 2.2*	80.0 ± 6.2*	121.8 ± 6.4
100 μM	80.2 ± 1.7	104.1 ± 1.5	145.0 ± 7.3*	19.3 ± 1.9**	45.5 ± 4.2#	106.9 ± 6.5#	184.8 ± 12.8**
Washout	81.7 ± 1.9	104.0 ± 1.2	165.5 ± 7.0	8.6 ± 0.5	18.7 ± 1.7	76.2 ± 4.3*	105.5 ± 9.1
Papillary muscle (n = 11)							
Control	81.7 ± 1.2	100.5 ± 1.1	169.5 ± 5.6	9.9 ± 1.2	16.4 ± 1.2	68.4 ± 4.6	100.0 ± 0.0
Quinidine 75 μM	80.5 ± 1.3	94.7 ± 1.3**	80.7 ± 5.2#	18.7 ± 1.4#	33.7 ± 2.3#	109.5 ± 6.6#	84.6 ± 3.7**
Atrial strip (n = 9)							
Control	77.4 ± 1.2	87.8 ± 1.6	162.9 ± 6.4	2.4 ± 0.2	6.7 ± 0.5	46.3 ± 3.5	100.0 ± 0.0
CIJ-3-2F 10 μM	76.6 ± 1.4	85.5 ± 1.5	146.8 ± 8.1	3.1 ± 0.2*	8.5 ± 0.5	50.7 ± 3.7	104.3 ± 2.5
30 μM	75.9 ± 1.4	81.5 ± 2.0*	123.3 ± 9.7*	5.2 ± 0.5**	13.1 ± 1.3**	63.4 ± 4.1*	137.5 ± 9.6*
100 μM	73.6 ± 1.5	76.5 ± 2.0#	101.2 ± 10.8**	11.0 ± 1.7**	22.3 ± 2.7**	79.1 ± 6.0#	197.9 ± 18.5**
Washout	77.0 ± 1.6	86.7 ± 1.3	151.2 ± 5.1	3.2 ± 0.3	9.4 ± 1.2	50.8 ± 5.2	105.1 ± 3.2

Values are expressed as mean ± SEM. RMP, resting membrane potential; APA, action potential amplitude; V_{max}, maximal upstroke velocity of phase 0 depolarization; APD_{25}, APD_{50} and APD_{90}, action potential duration measured at 25, 50 and 90% repolarization respectively; CF, contractile force. The basal values of CF in papillary muscles treated with CIJ-3-2F and quinidine were 0.61 ± 0.12 mN (n = 11) and 0.45 ± 0.05 mN (n = 11), respectively, and in left atrial strips treated with CIJ-3-2F was 0.22 ± 0.06 mN (n = 9). *P < 0.05, **P < 0.01, #P < 0.001; significantly different from control.

Time-dependent inhibition of I_{to} by CIJ-3-2F. As shown in Figure 6E, in the presence of CIJ-3-2F the decay of I_{to} was accelerated in a concentration-dependent manner. At +60 mV, the decay of I_{to} under control conditions was well fitted to a mono-exponential function. However, the time course of decay in the presence of CIJ-3-2F (≧1 μM) was bi-exponential. CIJ-3-2F decreased the fast time constant (τ_1) of current decay in a concentration-dependent manner (Table 5). To test whether the acceleration of I_{to} decay induced by CIJ-3-2F might be associated with time-dependent block of the open channel, the fractional block of I_{to} was plotted as a function of time after the start of depolarization (Figure 7A). Block was found to develop in a time-dependent fashion, with an exponential onset as shown by the curve fits in the figure. At 1, 3 and 10 μM CIJ-3-2F, the average maximum inhibition were 35 ± 3, 56 ± 3 and 80 ± 2% and the time constants for the developing block (τ_B) were 11.9 ± 3.0, 7.6 ± 1.9 and 4.2 ± 1.2 ms (n = 9) respectively. Figure 7B shows that the relationship between $1/\tau_B$ and the drug concentration was well described by a linear equation. The result of this analysis gave an apparent association rate constant k_{+1} = 27.2 ± 6.3 μM^{-1}·s^{-1} and a dissociation rate constant k_{-1} = 94.4 ± 14.6 s^{-1}. The estimated equilibrium dissociation constant K_D (k_{-1}/k_{+1}) was 4.6 ± 0.8 μM (n = 9), a value in good agreement with the IC_{50} value of 4.4 ± 1.0 μM calculated from the concentration-response curve.

Effects of CIJ-3-2F on voltage-dependent steady-state activation and inactivation and recovery from inactivation of I_{to} channel. The voltage dependence of the conductance variable ($G_{to}/G_{to,\ max}$) of I_{to} activation was determined from I–V relationships shown in Figure 6B. The resultant curves were fitted by the Boltzmann equation to estimate half-activation potential (V_h) and slope (k) (Figure 7D). CIJ-3-2F had no effect on the V_h and k of the activation curve (Table 5). The voltage dependence of steady-state inactivation was determined with the double-pulse protocol as shown in the inset of Figure 7C. A family of current traces is shown for control conditions in Figure 7C. The relative amplitudes of I_{to} ($I_{to}/I_{to,\ max}$) were plotted against prepulse potentials and also fitted to the Boltzmann distribution. CIJ-3-2F had no effect on the steady-state inactivation relationship (Figure 7D and Table 5). The time course of recovery from CIJ-3-2F-induced inhibition of I_{to} channels was determined using a paired-pulse protocol (Figure 7E, inset). The predrug superimposed currents are illustrated in Figure 7E. Recovery curves in the absence and presence of 1 μM CIJ-3-2F were well fitted by a mono-exponential function. However, recovery in concentrations greater than 1 μM was better described by the sum of bi-exponentials (Figure 7F, Table 5). Thus, CIJ-3-2F retarded the time course of recovery from inactivation of I_{to}.

Frequency and use dependence of I_{to} inhibition. The use-dependent blockade of I_{to} by CIJ-3-2F was determined at 0.33,

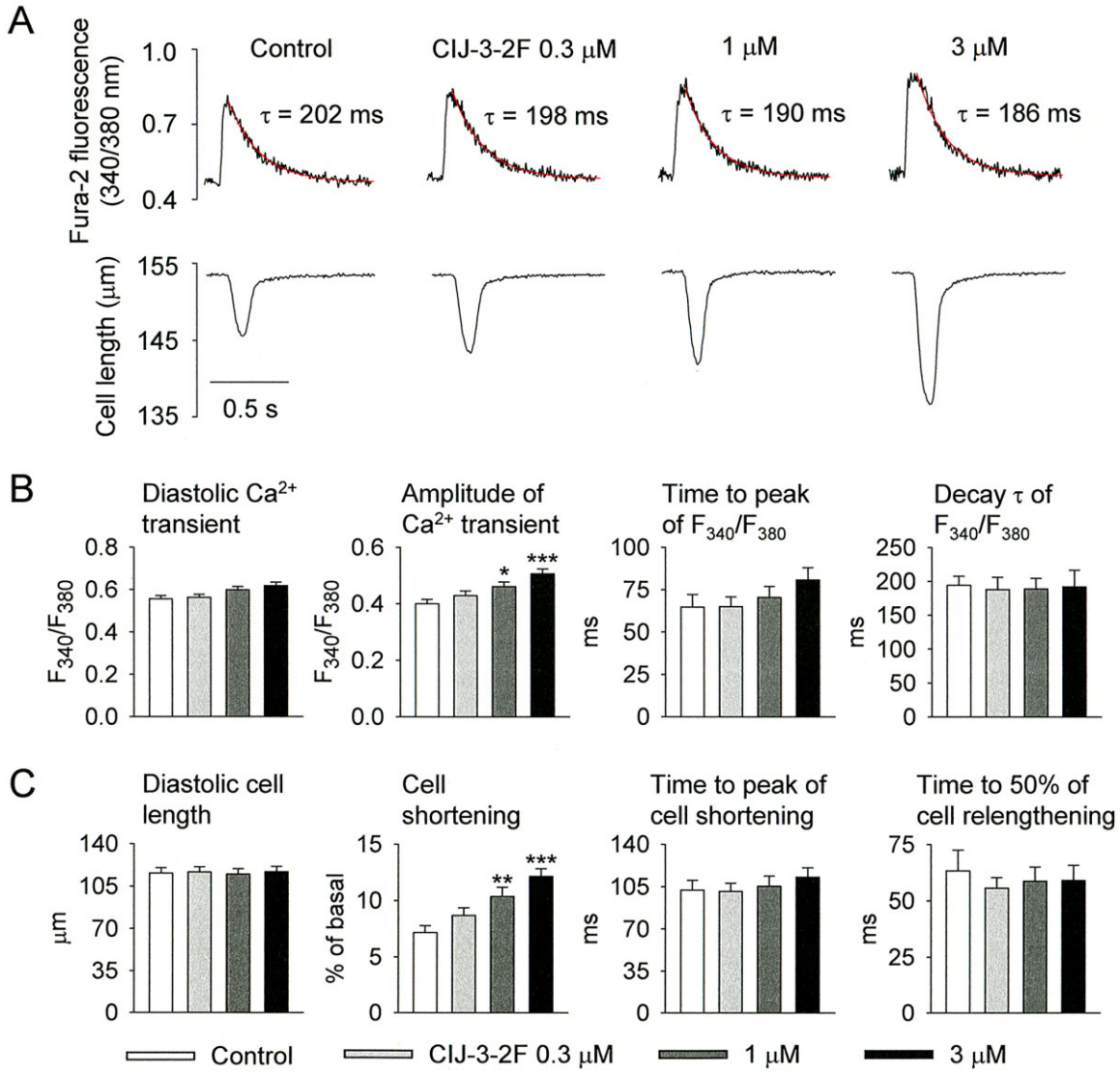

Figure 4

Effects of CIJ-3-2F on Ca^{2+} transients and cell shortening in rat ventricular myocytes. (A) Representative recordings of Ca^{2+} transients (fura-2 fluorescence ratio F_{340}/F_{380}, upper tracings) with fitted curves and the corresponding cell shortening (lower tracings) before and after applications of 0.3, 1 and 3 μM CIJ-3-2F. The myocyte was stimulated at 1 Hz. (B,C) Bar graphs showing the averaged data of the effects of CIJ-3-2F on parameters of Ca^{2+} transients and cell shortening respectively. Cell shortening is normalized to resting cell length. Data are mean ± SEM from 21 experiments. *P < 0.05, **P < 0.01, ***P < 0.001; significantly different from control.

1 and 2 Hz using a train of 16 depolarizing pulses (inset of Figure 7G). Figure 7G shows the I_{to} traces recorded at 2 Hz in the absence and presence of 3 μM CIJ-3-2F. Under control conditions, the peak current amplitude produced by each pulse remained constant during a train of 16 pulses. Following application of CIJ-3-2F, the current amplitude produced by the first pulse was slightly reduced, and the current amplitude declined with successive pulses and reached a steady level. The I_{to} amplitude for each pulse at each frequency was normalized to that of control in the first pulse at 0.33 Hz and plotted as a function of pulse number (Figure 7H). In the absence of the drug, the normalized peak I_{to} amplitudes of the 16th pulse at 0.33, 1 and 2 Hz were 97 ± 2%, 100 ± 1% and 98 ± 3% (n = 8) of those of the first pulse respectively. In the presence of CIJ-3-2F (3 μM), the corresponding values were 96 ± 2% (P > 0.05), 89 ± 2% (P < 0.01) and 68 ± 3% (P < 0.001, n = 8).

Effects of CIJ-3-2F on sodium inward current (I_{Na})

The time course of I_{Na} (at –20 mV) recorded in a ventricular cell in the absence and presence of CIJ-3-2F is shown in Figure 8A. The inhibitory effect of CIJ-3-2F reached steady state within 3–5 min and was partially reversed upon washout. The concentration-response curve of the effect of CIJ-3-2F on peak I_{Na} is shown in Figure 8B. The calculated IC_{50}

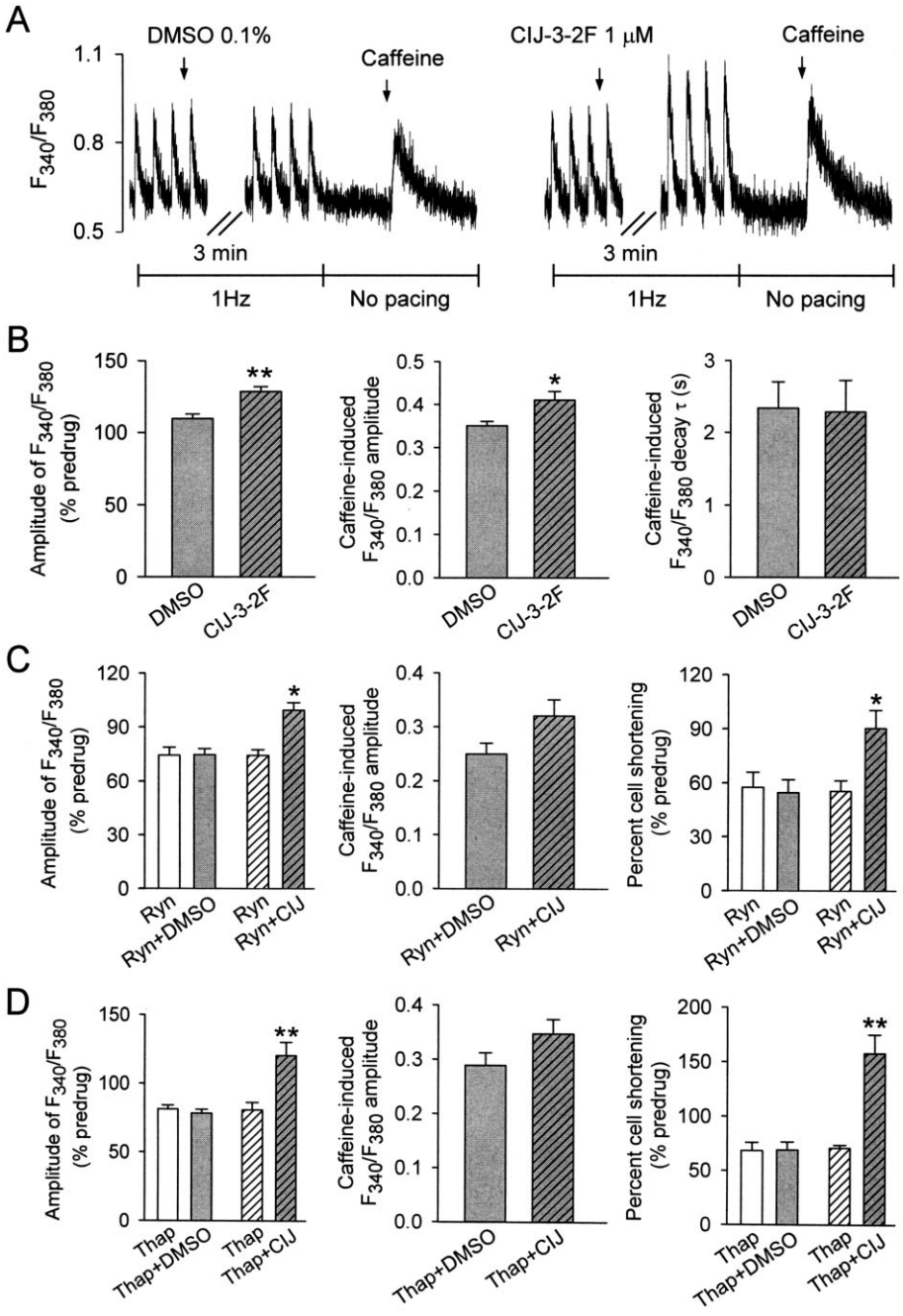

Figure 5

(A) Representative recordings of caffeine-induced Ca^{2+} transients (F_{340}/F_{380}) in a rat ventricular myocyte before and after application of vehicle (0.1% DMSO; left panel) or 1 μM CIJ-3-2F (right panel). A local caffeine concentration of 10 mM was achieved within 5 s. (B) Bar graphs showing the averaged data of the effects of vehicle (0.1% DMSO, $n = 11$) or CIJ-3-2F ($n = 12$) on the amplitude of electrically induced Ca^{2+} transients (left) and the amplitude (middle) and decay time constant (τ) of the caffeine-induced Ca^{2+} transients (right). $^*P < 0.05$, $^{**}P < 0.01$; significantly different from DMSO control. (C) Averaged data of the effects of vehicle (0.1% DMSO, $n = 10$) or CIJ-3-2F ($n = 12$) on the amplitudes of electrically induced (left) and caffeine-induced Ca^{2+} transients (middle), and cell shortening (right) in the presence of ryanodine (Ryn, 0.5 μM). $^*P < 0.05$; significantly different from Ryn + DMSO group. (D) Averaged data of the effects of vehicle (0.1% DMSO, $n = 9$) or CIJ-3-2F ($n = 9$) on the amplitudes of electrically induced (left) and caffeine-induced Ca^{2+} transients (middle), and cell shortening (right) in the presence of thapsigargin (Thap, 0.5 μM). $^{**}P < 0.01$; significantly different from Thap + DMSO group. Myocytes were incubated with ryanodine or thapsigargin for 3 min and then vehicle or CIJ-3-2F was added for further 3 min. All data are expressed as mean ± SEM.

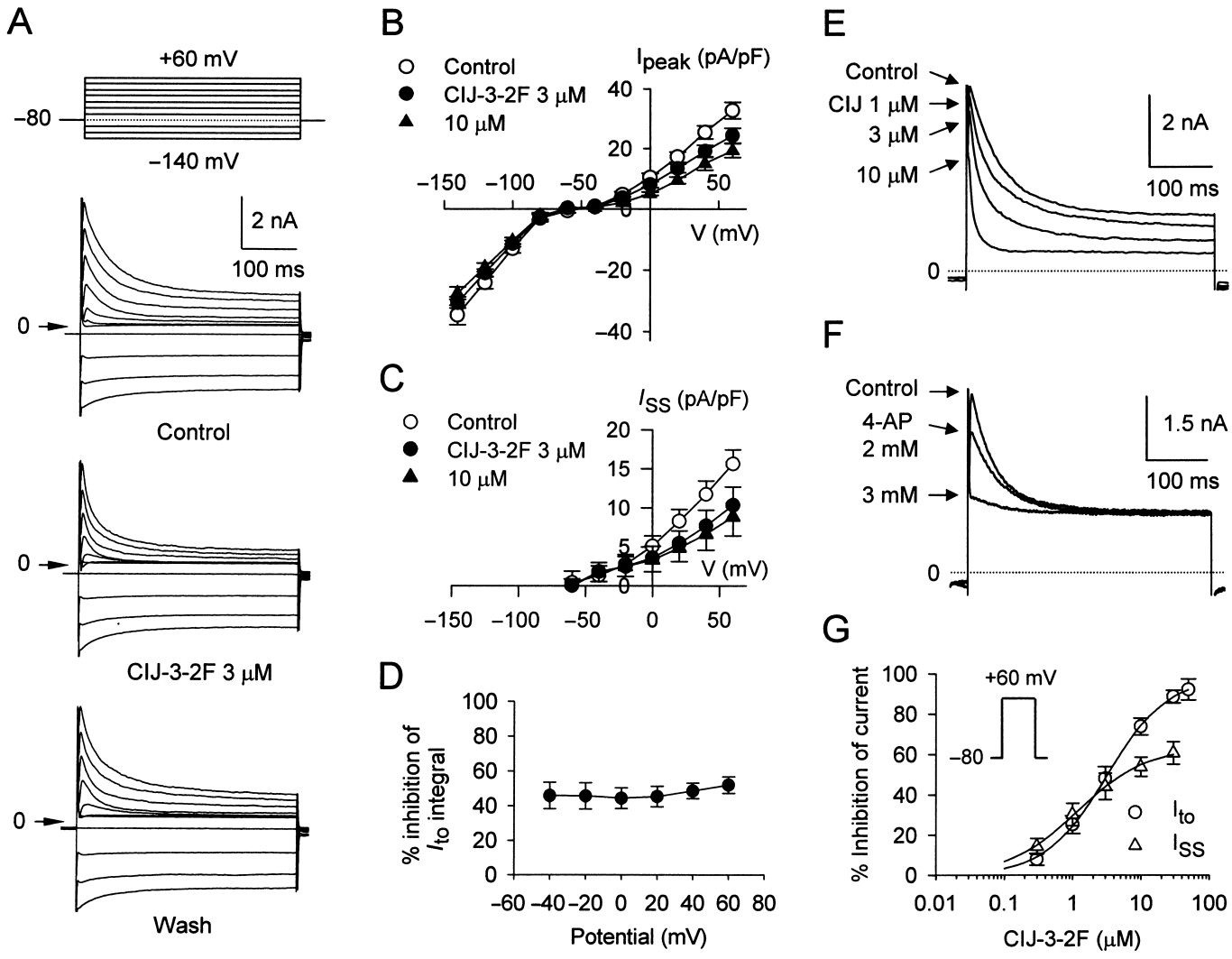

Figure 6

Effects of CIJ-3-2F on K^+ currents in rat ventricular myocytes. (A) Family of current traces obtained by applying a series of 400 ms long voltage pulses from –140 to +60 mV from a holding potential of –80 mV with a stimulation frequency of 0.2 Hz in the absence and presence of 3 and 10 μM CIJ-3-2F. (B) Averaged *I–V* relationships for I_{to} and I_{K1} peak currents observed in the absence and presence of CIJ-3-2F. I_{to} was measured as the difference between the peak current and the steady-state current (I_{ss}) at the end of the pulse. Data points are mean ± SEM (n = 10). (C) Averaged *I–V* relationships for I_{ss} observed in the absence and presence of CIJ-3-2F (n = 10). (D) Percent inhibition of the integral of I_{to} following exposure to 3 μM CIJ-3-2F plotted as a function of test potential. As CIJ-3-2F accelerated the decay time course of I_{to}, the reduction in I_{to} was quantified from the integral of the inactivating current. Data points are mean ± SEM (n = 10). (E) The original recordings of I_{to} and I_{ss} generated by 400 ms depolarizing pulses to +60 mV from a holding potential of –80 mV under control conditions and in the presence of increasing concentrations of CIJ-3-2F (1–10 μM). (F) Superimposed records of I_{to} and I_{ss} elicited by a protocol as described in panel E in the absence and presence of 4-AP. 4-AP at 2 and 3 mM decreased I_{to} amplitude by 30 ± 4 and 83 ± 5% (n = 5) respectively. (G) Concentration-response curves for the inhibition of CIJ-3-2F on the integral of I_{to} (n = 9) and the amplitude of I_{ss} (n = 9) at +60 mV. Percentage inhibition of current was plotted against drug concentration. Continuous lines were drawn according to the fitting of Hill equation.

was 2.8 ± 0.4 μM with an E_{max} of 98.8 ± 4.6% (n_H = 1.29 ± 0.12, n = 13). The decay of I_{Na} at –20 mV was best fitted by the sum of bi-exponential functions. Application of 3 μM CIJ-3-2F had no significant effect on either the fast or the slow time constants (Table 5). Figure 8C and D show the superimposed I_{Na} currents and the *I–V* relationships for I_{Na} respectively. CIJ-3-2F reduced the current amplitude but did not alter the shape of the *I–V* relationship. CIJ-3-2F had no effect on the voltage dependence for activation of I_{Na} (Figure 8E, Table 5). In contrast, CIJ-3-2F (>1 μM) caused a negative shift in steady-state inactivation without affecting the slope factor (k) (Figure 8E, Table 5). Recovery of I_{Na} from inactivation was assessed using a paired-pulse protocol (Figure 8F). Under control conditions, I_{Na} recovered rapidly, and the time course of this recovery was well described by the sum of bi-exponentials. CIJ-3-2F produced prolongation of both τ_f and τ_s with no effect on the proportion of the fast component (A_f) of the recovering current (Table 5).

Table 5

Kinetic parameters of the voltage dependence of steady-state activation and inactivation, and recovery from inactivated state of I_{to}, Ca^{2+} and Na^{+} channels under the influence of CIJ-3-2F

			Control	CIJ-3-2F (μM)		
		n		1	3	10
I_{to}						
Decay	τ_1 (ms)	10	43.5 ± 1.9	22.8 ± 2.3#	14.0 ± 1.4#	10.6 ± 1.5#
	τ_2 (ms)	10	–	93.9 ± 7.4	85.9 ± 7.0	78.2 ± 13.7
Activation	V_h (mV)	10	−3.9 ± 3.2	−4.2 ± 2.1	−2.6 ± 3.0	−2.6 ± 4.4
	k (mV)	10	16.4 ± 1.4	16.5 ± 1.2	17.5 ± 1.7	19.2 ± 1.8
Inactivation	V_h (mV)	9	−38.2 ± 2.5	−38.5 ± 2.0	−38.4 ± 2.0	−38.0 ± 2.3
	k (mV)	9	−4.8 ± 0.3	−5.2 ± 0.5	−6.2 ± 0.4	−6.1 ± 0.8
Recovery	τ_f (ms)	9	44.9 ± 5.3	58.6 ± 6.2	43.3 ± 6.8	52.1 ± 10.0
	τ_s (ms)	9	–	–	519.4 ± 139.4	727.3 ± 213.9
I_{Na}						
Decay	τ_1 (ms)	12	1.35 ± 0.19	1.42 ± 0.21	1.54 ± 0.22	–
	τ_2 (ms)	12	7.26 ± 0.68	8.06 ± 0.69	8.46 ± 0.89	–
Activation	V_h (mV)	8	−44.7 ± 1.7	−44.8 ± 1.3	−45.1 ± 1.9	–
	k (mV)	8	4.2 ± 0.3	4.3 ± 0.2	4.5 ± 0.2	–
Inactivation	V_h (mV)	9	−75.9 ± 1.4	−80.3 ± 2.6	−85.9 ± 2.9*	−93.9 ± 3.1#
	k (mV)	9	−5.9 ± 0.3	−5.9 ± 0.3	−6.1 ± 0.4	−5.9 ± 0.2
Recovery	A_f	8	0.80 ± 0.07	0.77 ± 0.04	0.75 ± 0.09	0.73 ± 0.05
	τ_f (ms)	8	41.9 ± 9.3	59.3 ± 19.9	122.4 ± 38.3	150.1 ± 36.6
	τ_s (ms)	8	190.3 ± 36.4	264.2 ± 82.6	457.9 ± 100.6	538.5 ± 85.3*
$I_{Ca,L}$						
Decay	τ_1 (ms)	13	20.8 ± 2.6	22.5 ± 2.7	23.4 ± 3.8	24.0 ± 4.2
	τ_2 (ms)	13	92.0 ± 10.0	90.1 ± 7.7	91.1 ± 11.2	92.3 ± 9.5
Activation	V_h (mV)	9	−17.4 ± 0.8	−15.8 ± 1.7	−16.2 ± 1.9	−16.6 ± 2.4
	k (mV)	9	4.8 ± 0.7	4.7 ± 0.4	4.9 ± 0.5	4.8 ± 0.6
Inactivation	V_h (mV)	9	−29.3 ± 1.6	−36.3 ± 1.0*	−47.6 ± 3.2**	−56.3 ± 2.2#
	k (mV)	9	−5.7 ± 0.4	−6.1 ± 0.7	−6.9 ± 1.0	−7.6 ± 0.4
Recovery	A_f	8	0.60 ± 0.08	0.49 ± 0.08	0.44 ± 0.04	0.33 ± 0.06*
	τ_f (s)	8	0.16 ± 0.03	0.16 ± 0.04	0.24 ± 0.04	0.25 ± 0.06
	τ_s (s)	8	1.34 ± 0.39	1.16 ± 0.29	1.72 ± 0.22	2.19 ± 0.14

Data are expressed as mean ± SEM. *n* is number of experiments. τ_1 and τ_2 indicate fast and slow time constant for channel inactivation respectively. V_h and *k* indicate half-activation or inactivation voltage and slope factor. A_f indicates the fast fraction of channel recovery. τ_f and τ_s indicate fast and slow time constant for channel recovery respectively. *$P < 0.05$, **$P < 0.01$, #$P < 0.001$; significantly different from control.

To study the use-dependent I_{Na} block, myocytes were stimulated by a 16 pulse train at varying rates (1 to 4 Hz) (Figure 8G). Under control conditions, the normalized peak I_{Na} amplitudes of the 16th pulse at 1 and 4 Hz were 97 ± 1% and 90 ± 1% (n = 8) of those of the first pulse respectively. Following application of CIJ-3-2F, the current amplitude produced by the first pulse of the train was significantly reduced, a characteristic of tonic block. CIJ-3-2F also caused a pronounced use-dependent block of I_{Na}. In the presence of 3 μM CIJ-3-2F, the normalized current amplitudes of the 16th pulse at 1 and 4 Hz were 92 ± 1% ($P < 0.05$ vs. control) and 57 ± 3% ($P < 0.001$, n = 8) of those of the first pulse respectively.

In rat atrial myocytes, CIJ-3-2F caused a more potent inhibition of I_{Na} than that seen in ventricular myocytes (Supporting Information Figure S4B).

Effects of CIJ-3-2F on L-type calcium current ($I_{Ca,L}$)

Figure 9A illustrates the original $I_{Ca,L}$ recordings obtained before, after the addition and after the washout of CIJ-3-2F (10 μM) in a ventricular myocyte. The average *I–V* curves of $I_{Ca,L}$ are plotted in Figure 9B. CIJ-3-2F decreased $I_{Ca,L}$ amplitude in a concentration-dependent manner and the effect was partly reversible. The concentration–response relationship for the inhibition of $I_{Ca,L}$ by CIJ-3-2F was evaluated at 0 mV

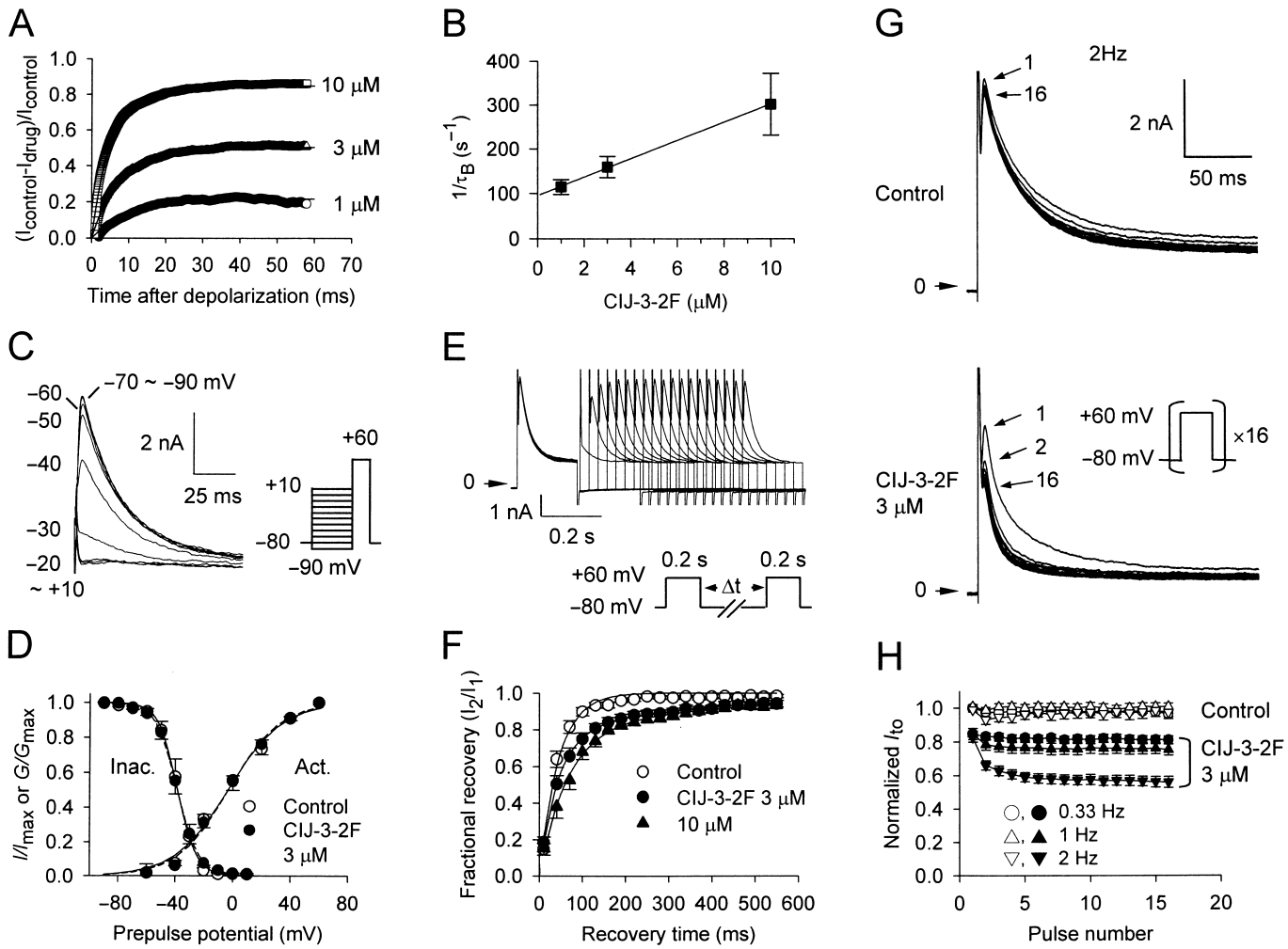

Figure 7

Effects of CIJ-3-2F on kinetic properties of I_{to} in rat ventricular myocytes. (A) Time course of the development of I_{to} inhibition by 1, 3 and 10 μM CIJ-3-2F. This graph was determined from the original traces in Figure 5E. The reduction of I_{to} in the presence of CIJ-3-2F is expressed as a proportion of the control current at any given time after the start of the depolarizing pulse. The curves are a simultaneous fit of mono-exponential equation of the form: $B = B_{max}\,[1 - \exp(-t/\tau_B)]$, where B_{max} equals maximum block and B equals the amount of block at time t. The time constants for the onset of block (τ_B) at 1, 3 and 10 μM CIJ-3-2F were 10.4, 7.5 and 5.2 ms respectively. (B) Rate of block ($1/\tau_B$) of I_{to} as a function of drug's concentration ([D]). The line is a regression fit of the following equation: $1/\tau_B = k_{+1}[D] + k_{-1}$, where k_{+1} and k_{-1} are the association and dissociation rate constants for the drug respectively. Data shown are mean ± SEM ($n = 9$). (C) Traces of voltage dependence of I_{to} inactivation elicited by the second pulse of the double-pulse protocol (inset) under control conditions. A conditioning pulse (400 ms long) to potentials ranging from −90 to +10 mV was applied before a 200 ms test pulse to +60 mV. The holding potential was −80 mV. (D) Voltage dependence of steady-state I_{to} inactivation (Inac., $n = 9$) and activation (Act., $n = 10$) in the absence and presence of 3 μM CIJ-3-2F. Line curves shown were fits of mean data by Boltzmann distribution. (E) Representative current traces of time-dependent recovery of I_{to} from inactivation. A 200 ms prepulse (P_1) was first applied from a holding potential of −80 mV to +60 mV, which was followed by a 200 ms test pulse (P_2) after variable interpulse intervals ranging from 10 to 550 ms (inset). Each paired-pulse sequence was separated by a 10 s interval. (F) Mean data for time course of recovery of I_{to} from inactivation in the absence and presence of 3 and 10 μM CIJ-3-2F in nine cells. The normalized recovery fraction of I_{to} (I_2/I_1) was plotted against the recovery times. Data were best-fits of single- (control) or bi-exponential (CIJ-3-2F) functions. (G) Use- and frequency-dependent effects of CIJ-3-2F on I_{to}. A train of 400 ms depolarizing pulses was applied at 2 Hz from a holding potential of −80 mV to +60 mV first under control conditions (upper panel) and then at 3 min after superfusion with 3 μM CIJ-3-2F (lower panel). The cells were rested for 1 min before the train of pulses was applied. (H) Averaged data for pulse train frequencies of 0.33, 1 and 2 Hz. Amplitudes of I_{to} were normalized to that elicited by the first pulse before drug application at 0.03 Hz and plotted against the pulse number in the absence and presence of CIJ-3-2F (3 μM). Each data point represents mean ± SEM ($n = 8$).

(Figure 9C). The IC_{50} was 4.9 ± 1.3 μM with an E_{max} of 69.4 ± 4.4 % ($n_H = 1.24 \pm 0.15$, $n = 10$). The time course of inactivation of $I_{Ca,L}$ at 0 mV was well fitted to a bi-exponential function and was not significantly changed by CIJ-3-2F (Table 5). CIJ-3-2F did not affect the voltage dependence of activation of $I_{Ca,L}$, whereas it significantly shifted the steady-state inactivation towards negative potentials (Figure 9D, Table 5). Recovery of $I_{Ca,L}$ from inactivation was fitted to a

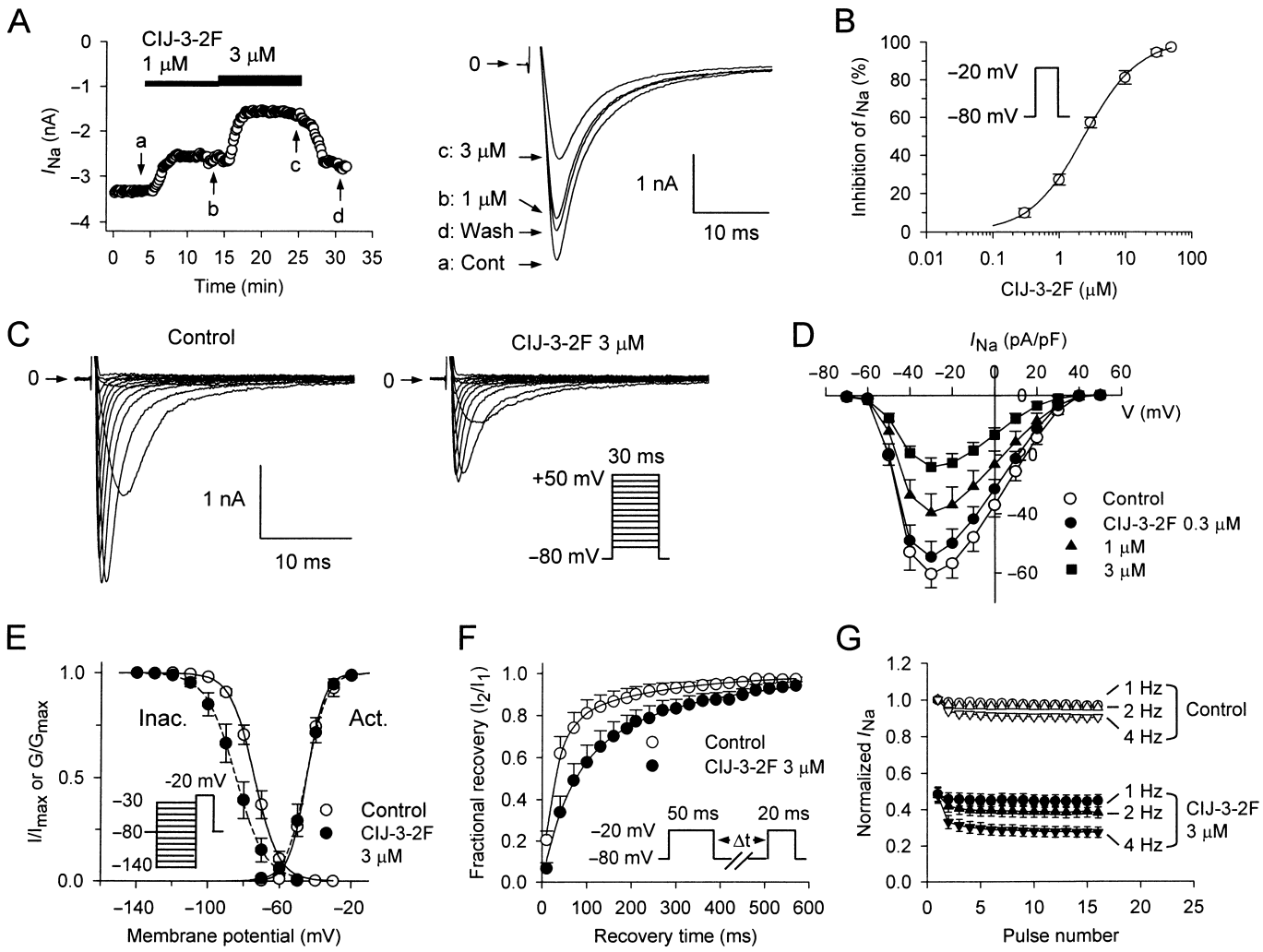

Figure 8

Effects of CIJ-3-2F on I_{Na} in rat ventricular myocytes. (A) Time-dependent effect of 1 and 3 μM CIJ-3-2F on I_{Na} elicited by 30 ms long voltage step to −20 mV from a holding potential of −80 mV (panel B inset) delivered every 10 s. The original superimposed I_{Na} traces at corresponding time points are shown in the right inset. (B) Concentration-response curve of I_{Na} inhibition by CIJ-3-2F at −20 mV (n = 13) was fitted to a Hill equation. (C) Superimposed traces of I_{Na} elicited by 30 ms step pulses between −70 mV and +50 mV from a holding potential of −80 mV (inset) under control conditions and after 5 min superfusion with 3 μM CIJ-3-2F. (D) Averaged I–V relationships of I_{Na} in the absence and presence of 0.3, 1 and 3 μM CIJ-3-2F (n = 8). (E) Voltage dependence of inactivation (Inac., n = 9) and activation (Act., n = 8) of I_{Na} in the absence and presence of 3 μM CIJ-3-2F. The activation curves were derived using I–V curves shown in panel D. Steady-state inactivation was examined with a double-pulse protocol shown in the inset: a 1 s conditioning pulse to various potentials ranging from −140 to −30 mV was applied from the holding potential of −80 mV, which was followed by a 50 ms long test pulse to −20 mV. Line curves shown are fits of mean data by Boltzmann distribution. (F) Recovery of I_{Na} from inactivation was determined using a paired-pulse protocol (inset) in the presence and absence of 3 μM CIJ-3-2F. The recovery curves were fitted to bi-exponential functions. Each data point represents mean ± SEM from eight cells. (G) Tonic- and use-dependent block of I_{Na} by CIJ-3-2F. I_{Na} were elicited by a train of 16 consecutive step pulses of 20 ms to −20 mV from a holding potential of −80 mV at 1, 2 or 4 Hz after a 1 min rest. Amplitudes of I_{Na} were normalized to that elicited by the first pulse before drug application at 1 Hz and plotted against the pulse number in the absence and presence of CIJ-3-2F (3 μM). Each data point represents mean ± SEM (n = 8).

bi-exponential function (Figure 9E). CIJ-3-2F (3 and 10 μM) retarded the recovery of $I_{Ca,L}$ by reducing the fraction of the fast component of the recovery current (A_f) (Table 5). Both the fast (τ_f) and slow recovery time constant (τ_s) showed a trend to be increased by CIJ-3-2F, but this change did not reach statistical significance. And in atrial myocytes, CIJ-3-2F produced a similar extent of inhibition on $I_{Ca,L}$ to that seen in ventricular myocytes (Supporting Information Figure S4C).

Discussion

The major finding of this study is that acute application of CIJ-3-2F resulted in significant antiarrhythmic effects with low levels of proarrhythmic actions in isolated hearts from male or female rats. The antiarrhythmic action may be mediated through blockade mainly of the Na^+ and I_{to} channels, but also of the Ca^{2+} and I_{ss} channels both in atrial and ventricular

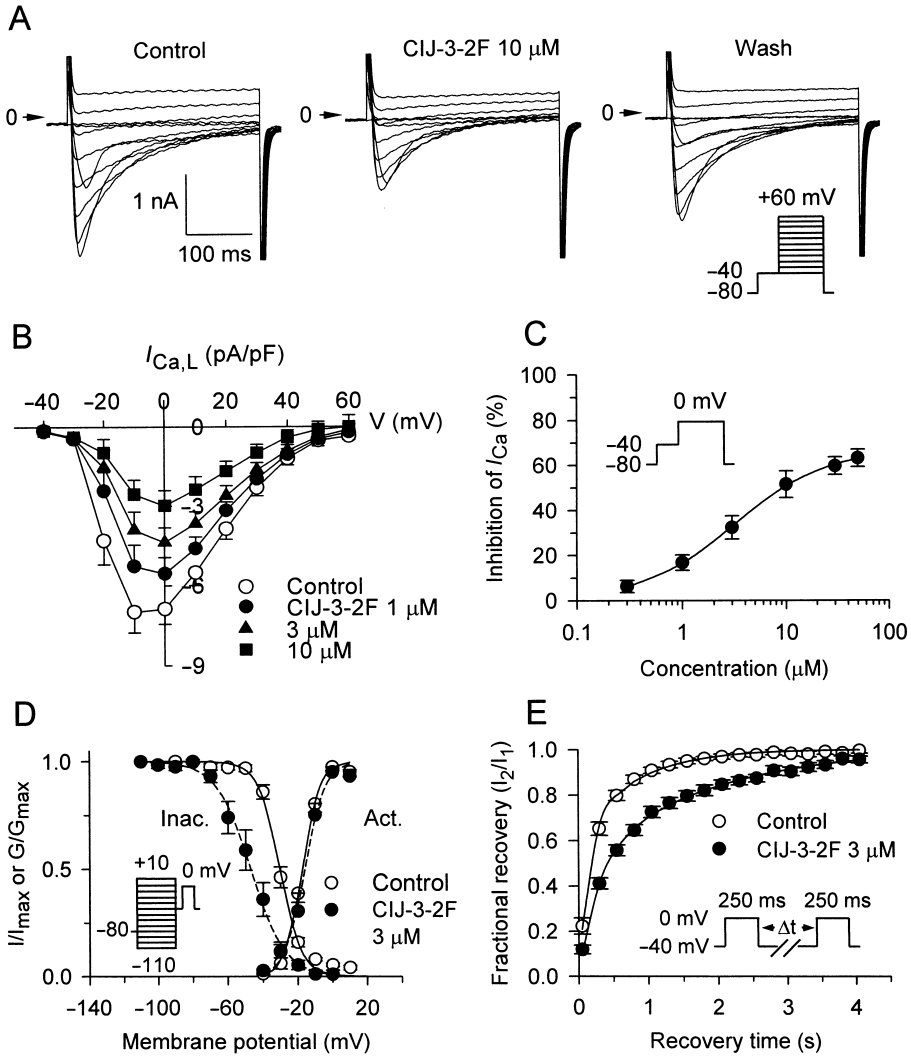

Figure 9

Effects of CIJ-3-2F on $I_{Ca,L}$ in rat ventricular myocytes. (A) Family of current traces obtained by applying a series of 300 ms long step pulses between –40 mV and +60 mV from a holding potential of –80 mV, after a prepulse to –40 mV to inactivate I_{Na} and T-type Ca^{2+} current, under control conditions and in the presence and after washout of 10 μM CIJ-3-2F. (B) Averaged *I–V* relationships of $I_{Ca,L}$ in the absence and presence of 1, 3 and 10 μM CIJ-3-2F. Each data point represents mean ± SEM from nine cells. (C) Concentration-response curve of $I_{Ca,L}$ inhibition by CIJ-3-2F at 0 mV ($n = 10$) was fitted to a Hill equation. (D) Voltage dependence of inactivation (Inac., $n = 9$) and activation (Act., $n = 8$) of $I_{Ca,L}$ in the absence and presence of 3 μM CIJ-3-2F. Steady-state inactivation was examined with a double-pulse protocol (inset): 1 s conditioning pulses were applied in 10 mV steps between –110 mV and +10 mV from a holding potential of –80 mV, and then the test pulse of 200 ms duration was applied to 0 mV (interpulse duration was 30 ms). Line curves shown are fits of mean data by Boltzmann distribution. (E) Recovery of $I_{Ca,L}$ from inactivation was determined with the paired-pulse protocol as shown in the inset. The recovery curves were fitted with a bi-exponential function. Each data point represents mean ± SEM from seven cells.

myocytes, although only the effects on ventricular myocytes from male rats were examined in detail in this study (channel nomenclature follows Alexander *et al.*, 2013). Consequently, CIJ-3-2F prolonged the conduction interval and the refractoriness of the cardiac conduction system and myocardial tissues.

An important consequence of both myocardial ischaemia and reperfusion is the occurrence of various cardiac arrhythmias. The mechanisms underlying the initiation of serious ventricular arrhythmias during both ischaemia and reperfusion are complex and the ultimate electrophysiological disturbances may include the establishment of re-entry circuits and enhanced automaticity such as oscillatory afterpotentials (Manning and Hearse, 1984; Pogwizd and Corr, 1987; Curtis and Hearse, 1989b). In this study, we have provided evidence that CIJ-3-2F can reduce the incidences of ischaemic and reperfusion-induced arrhythmias probably by suppression of oscillatory afterpotentials or extrasystole by blocking Na^+ or Ca^{2+} channels or by termination of a re-entry circuit by blocking K^+ channels. In addition, the increase of coronary flow induced by CIJ-3-2F may contribute to the delay in arrhythmia onset (Tsuchihashi and Curtis, 1991).

Atrial tachyarrhythmias such as atrial flutter or fibrillation induced by electrical pacing are known to be generated, at least in part, by a re-entrant mechanism (Nattel, 2002). Our results demonstrated that CIJ-3-2F prevented experimentally induced atrial tachyarrhythmias, probably by prolonging the AERP mainly through the blockade of K^+ channels, thus inhibiting re-entry. In addition, the inhibition of I_{Na} by CIJ-3-2F may destabilize re-entrant rotors and break up arrhythmic circuits by reducing impulse conduction velocity and tissue excitability (Wijffels *et al.*, 2000; Kneller *et al.*, 2005).

Voltage-gated K^+ channels play a crucial role in determining resting potential and the shape and duration of the cardiac action potential. The I_{to} is generally considered an important repolarizing current in the action potential of several mammalian tissues, including human atrium and ventricle (Escande *et al.*, 1987; Näbauer *et al.*, 1993) and rat cardiac tissues (Josephson *et al.*, 1984). Our results showed that the dominant I_{to} responsible for the early phase of repolarization of the rat action potential and the I_{ss}, which we ascribed to a delayed rectifier K^+ current, were differentially blocked by CIJ-3-2F. Thus suppression of these currents prolongs the APD and thus increases the refractoriness of the conduction system and the atrial and ventricular myocardium as observed with class III and some class I antiarrhythmic agents (Singh and Nademanee, 1985; Hondeghem, 1992).

Blockade of I_{to} by CIJ-3-2F was characterized by a moderate voltage-independent decrease in peak current and an apparent increase in the rate of current decay. The acceleration of I_{to} decay might be explained by a drug-induced acceleration of the normal conversion of open channels to an inactivated state. A more likely explanation, however, is that CIJ-3-2F binds preferentially to open state channels, as observed with quinidine, flecainide and propafenone (Slawsky and Castle, 1994; Clark *et al.*, 1995; Gross and Castle, 1998). At the onset of a depolarizing pulse, there was no inhibition of I_{to}, indicating that CIJ-3-2F may not bind to the resting channel. However, upon continued depolarization (i.e. during channel opening), blockade develops in an exponential manner. The estimated K_D value (~4.6 μM) for the time-dependent block by CIJ-3-2F is very close to the IC_{50} value (~4.4 μM) obtained from the concentration-response curve, a characteristic feature of open channel block (Jeong *et al.*, 2011). As the steady-state activation curve of I_{to} was not affected significantly by CIJ-3-2F, the inhibitory effect on I_{to} is the result of a change in conductance, but not in the gating mechanism. In comparison with the effect of its parent compound acrophyllidine, which exhibits a comparable potency on I_{to} (IC_{50} = 4.5 μM) with a remarkable negative shift in the voltage-dependent inactivation (Chang *et al.*, 2000), CIJ-3-2F had no effect on the inactivation curve, suggesting that it may not bind to the inactivated channel. Myocytes exposed to CIJ-3-2F exhibited both a fast and a slow component of I_{to} recovery after inactivation. The appearance of a slower component of recovery may result from the slower dissociation of this agent from its binding sites similar to the mode of action of quinidine (Clark *et al.*, 1995). This phenomenon may explain the observed use- and frequency-dependent block of I_{to} by this agent. The blocking effect of CIJ-3-2F on I_{to} is opposite from that of 4-AP, a commonly used blocker in which the blocking action preferentially occurs in the closed state and is relieved during the open state (Campbell *et al.*, 1993; Castle and Slawsky, 1993; Jahnel *et al.*, 1994).

The present study showed that CIJ-3-2F blocked Na^+ channels, a blockade that may contribute to its inhibition of the V_{max} of the action potential as well as to the prolongation of the conduction intervals and the refractoriness of the His-Purkinje system and myocardial tissues (Fozzard and Hanck, 1996). The RMP of atrial tissue is between –70 and –80 mV, a value more positive than that of the ventricle (Hume and Uehara, 1985). This property could explain the atrial selectivity of the suppression of the V_{max} and block of Na^+ channels. Our study showed that CIJ-3-2F inhibited I_{Na} with a negative shift of the voltage-dependent inactivation curve but did not alter the inactivation time constant. This effect may also account for the tonic block of CIJ-3-2F, although another possible mechanism is binding to resting state channels. CIJ-3-2F also caused use-dependent block and retardation of recovery from inactivation of Na^+ channels, as found with most class I agents (Clarkson *et al.*, 1988; Grant and Wendt, 1992). The marked use-dependent blockade of the Na^+ channel by CIJ-3-2F could be attributed to its slow dissociation from the inactivated channel. Overall, CIJ-3-2F may preferentially bind to the inactivated channel, resulting in a decrease of the available channels for activation (Hondeghem and Katzung, 1984). Under the pathological conditions associated with ischaemia, CIJ-3-2F may be especially effective at suppressing arrhythmias because partial membrane depolarization (Na^+ channel inactivation) occurs in ischaemic tissue (Shaw and Rudy, 1997).

Consistent with its modest depression of AV nodal conduction, CIJ-3-2F also prolonged the WCL and AV nodal ERP. This effect may result mainly from inhibition of $I_{Ca,L}$ as found with many typical class IV drugs (Talajic *et al.*, 1990). It is reasonable to speculate that the bradycardiac effect of CIJ-3-2F may also be mediated partially by an inhibition of the $I_{Ca,L}$. The present data showed that CIJ-3-2F caused a significant leftward shift of the steady-state inactivation curve and a delay in slow recovery kinetics of $I_{Ca,L}$ with no significant change in the steady-state activation curve, indicating that CIJ-3-2F can bind to the inactivated channels with a slow dissociation rate. Furthermore, the finding that CIJ-3-2F did not affect the inactivation rate of $I_{Ca,L}$ indicates that this agent seems unlikely to block the activated channels.

Drugs that block Ca^{2+} or Na^+ channels may result in a negative inotropic effect that is hazardous in some situations (Nawrath, 1981; Schlepper, 1989). Our results showed that CIJ-3-2F exhibited a moderate positive inotropic effect and an elevation of the $[Ca^{2+}]_i$ transient but no changes in its rising or decay kinetics. The time to peak of the $[Ca^{2+}]_i$ transient indicates the speed of Ca^{2+} release via ryanodine receptors from the SR, while the decay time constant reflects the rate of Ca^{2+} clearance from cytoplasm (Bouchard *et al.*, 1995). In rat cardiomyocytes, most (>90%) of the Ca^{2+} is taken back to the SR via the Ca^{2+}-ATPase pump. In the presence of caffeine, the extrusion of Ca^{2+} from the cytoplasm is mainly through the Na^+/Ca^{2+} exchanger. Our results showed that CIJ-3-2F still could increase the amplitude of Ca^{2+} transients in myocytes pretreated with SR blockers together with small changes in the kinetics of the $[Ca^{2+}]_i$ transient, suggesting that the action of CIJ-3-2F may not involve a direct interaction with the ryanodine receptor, SR Ca^{2+}-ATPase pump or Na^+/Ca^{2+}

exchanger. It has been proposed that the prolongation of APD may prolong the opening time of the L-type Ca^{2+} channel and lead to a greater Ca^{2+} entry via the Na^+/Ca^{2+} exchange working in the reverse mode, and thus may enhance cardiac contractility by increasing the amplitude of $[Ca^{2+}]_i$, either through the increase of SR Ca^{2+} loading, or increase of triggered Ca^{2+} release or both. (Bouchard *et al.*, 1995). This notion was further supported by the findings from some K^+ channel blockers, such as 4-AP (Bouchard *et al.*, 1995; Tahara *et al.*, 2001), and from rat myocytes following myocardial infarction (Sah *et al.*, 2001). In this context, the positive inotropic response of CIJ-3-2F could be ascribed to the prolongation of the APD and the subsequent increase of Ca^{2+} influx, which may overcome the moderate and direct inhibitory effect on Ca^{2+} channels and would result in an increased amount of Ca^{2+} remaining in the cytoplasm.

There are several limitations to this study that must be noted. As always, extrapolation of the results obtained from healthy rat heart to patients with cardiac disease must be approached with great caution. For example, there are marked differences in the shape and duration of the action potential in rat hearts compared with those in human hearts, especially in diseased states. In diseased hearts, the atrial or ventricular electrical remodelling can significantly affect the drug responses. Whether CIJ-3-2F could also be effective in chronic ischaemic disease models needs future studies. As mentioned above, the rat heart does not possess a functioning I_K current, and this would logically rule out any possible antiarrhythmic and/or proarrhythmic actions by a class III agent with potent I_{Kr} blocking activity. Although inhibition of depolarizing currents, especially I_{Na}, provides the probable explanation for the CIJ-3-2F-induced slowing of conduction in isolated hearts, it has been proposed that the decrease of gap junction coupling could markedly contribute to the conduction slowing (Kléber and Rudy, 2004). Additional studies are needed to examine the effect on gap junction conductance.

In summary, this study demonstrates that a benzyl-furoquinoline vasodilator, CIJ-3-2F, has atrial and ventricular antiarrhythmic activities, which are likely to result from its blockade of cardiac I_{to}, Na^+, I_{ss} and Ca^{2+} channels. CIJ-3-2F exhibits affinity for atrial tissues, which should provide more antiarrhythmic advantages over its parent compound, acrophyllidine. In fact, combinations of class III with class I and/or class IV features appear to be promising both in terms of antiarrhythmic activity and side effect minimization profiles (Mátyus *et al.*, 1997). Therefore, we suggest that CIJ-3-2F may be a very promising drug for the treatment of cardiac arrhythmias. The additional vasorelaxant and positive inotropic activities of this agent may be beneficial for patients with ventricular dysfunction.

Acknowledgements

The authors thank Hsiao-Yu Lee, Shi-Han Weng, Yu-Ting Liu and Chia-Ling Chen for technical help. This work was supported by grants from Chang Gung Medical Research Foundation (CMRP1293) and from the National Science Council of Taiwan (NSC96-2320-B-182-026-MY3).

Author contributions

G.-J. Chang conceived and designed the research. G.-J. Chang, Y.-H. Yeh, C.-J. Chang and W.-J. Chen conducted the experiments. G.-J. Chang and Y.-H. Yeh performed the data analysis. T.-P. Lin contributed the new reagents and materials. G.-J. Chang contributed to the writing of the manuscript.

Conflict of interest

None.

References

Alexander SPH, Benson HE, Faccenda E, Pawson AJ, Sharman JL, Catterall WA *et al.* (2013). The Concise Guide to PHARMACOLOGY 2013/14: Ion Channels. Br J Pharmacol 170: 1607–1651.

Amos GJ, Abrahamsson C, Duker G, Hondeghem L, Palmer M, Carlsson L (2001). Potassium and calcium current blocking properties of the novel antiarrhythmic agent H 345/52: implications for proarrhythmic potential. Cardiovasc Res 49: 351–360.

Bouchard RA, Clark RB, Giles WR (1995). Effects of action potential duration on excitation-contraction coupling in rat ventricular myocytes. Action potential voltage-clamp measurements. Circ Res 76: 790–801.

Bril A, Forest MC, Cheval B, Faivre JF (1998). Combined potassium and calcium channel antagonistic activities as a basis for neutral frequency dependent increase in action potential duration: comparison between BRL-32872 and azimilide. Cardiovasc Res 37: 130–140.

Campbell DL, Qu Y, Rasmusson RL, Strauss HC (1993). The calcium-independent transient outward potassium current in isolated ferret right ventricular myocytes. II. Closed state reverse use-dependent block by 4-aminopyridine. J Gen Physiol 101: 603–626.

Castle NA, Slawsky MT (1993). Characterization of 4-aminopyridine block of the transient outward current in adult rat ventricular myocytes. J Pharmacol Exp Ther 264: 1450–1459.

Chang GJ, Wu MH, Chen WP, Kuo SC, Su MJ (2000). The electrophysiological characteristics of the antiarrhythmic potential of acrophyllidine, an alkaloid isolated from *Acronychia halophylla*. Drug Dev Res 50: 170–185.

Chang GJ, Su MJ, Hung LM, Lee SS (2002). Cardiac electrophysiologic and antiarrhythmic actions of a pavine alkaloid derivative, *O*-methyl-neocaryachine, in rat heart. Br J Pharmacol 136: 459–471.

Chang GJ, Lin TP, Ko YS, Lin MS (2010). Endothelium-dependent and -independent vasorelaxation induced by CIJ-3-2F, a novel benzyl-furoquinoline with antiarrhythmic action, in rat aorta. Life Sci 86: 869–879.

Chang GJ, Chang CJ, Chen WJ, Yeh YH, Lee HY (2013). Electrophysiological and mechanical effects of caffeic acid phenethyl ester, a novel cardioprotective agent with antiarrhythmic activity, in guinea-pig heart. Eur J Pharmacol 702: 194–207.

Clark RB, Sanchez-Chapula J, Salinas-Stefanon E, Duff HJ, Giles WR (1995). Quinidine-induced open channel block of K^+ current in rat ventricle. Br J Pharmacol 115: 335–343.

Clarkson CW, Follmer CH, Ten Eick RE, Hondeghem LM, Yeh JZ (1988). Evidence for two components of sodium channel block by lidocaine in isolated cardiac myocytes. Circ Res 63: 869–978.

Curtis MJ, Hearse DJ (1989a). Reperfusion-induced arrhythmias are critically dependent upon occluded zone size: relevance to the mechanism of arrhythmogenesis. J Mol Cell Cardiol 21: 625–637.

Curtis MJ, Hearse DJ (1989b). Ischaemia-induced and reperfusion-induced arrhythmias differ in their sensitivity to potassium: implications for mechanisms of initiation and maintenance of ventricular fibrillation. J Mol Cell Cardiol 21: 21–40.

Curtis MJ, Hancox JC, Farkas A, Wainwright CL, Stables CL, Saint DA *et al.* (2013). The Lambeth Conventions (II): guidelines for the study of animal and human ventricular and supraventricular arrhythmias. Pharmacol Ther 139: 213–248.

Escande D, Coulombe A, Faivre J-F, Deroubaix E, Coraboeuf E (1987). Two types of transient outward currents in adult human atrial cells. Am J Physiol 252: H142–H148.

Faivre JF, Forest MC, Gout B, Bril A (1999). Electrophysiological characterization of BRL-32872 in canine Purkinje fiber and ventricular muscle. Effect on early after-depolarizations and repolarization dispersion. Eur J Pharmacol 383: 215–222.

Fozzard HA, Hanck DA (1996). Structure and function of voltage-dependent sodium channels: comparison of brain II and cardiac isoforms. Physiol Rev 76: 887–926.

Grant AO, Wendt DJ (1992). Block and modulation of cardiac Na^+ channels by antiarrhythmic drugs, neurotransmitters and hormones. Trends Pharmacol Sci 13: 352–358.

Gross GJ, Castle NA (1998). Propafenone inhibition of human atrial myocyte repolarizing currents. J Mol Cell Cardiol 30: 783–793.

Hondeghem LM (1992). Development of class III antiarrhythmic agents. J Cardiovasc Pharmacol 20 (Suppl. 2): S17–S22.

Hondeghem LM, Katzung BG (1984). Antiarrhythmic agents: the modulated receptor mechanism of action of sodium and calcium channel-blocking drugs. Annu Rev Pharmacol Toxicol 24: 387–423.

Hondeghem LM, Snyders DJ (1990). Class III antiarrhythmic agents have a lot of potential but a long way to go. Reduced effectiveness and dangers of reverse use dependence. Circulation 81: 686–690.

Hume JR, Uehara A (1985). Ionic basis of the different action potential configurations of single guinea-pig atrial and ventricular myocytes. J Physiol 368: 525–544.

Jahnel U, Klemm P, Nawrath H (1994). Different mechanisms of the inhibition of the transient outward current in rat ventricular myocytes. Naunyn Schmiedebergs Arch Pharmacol 349: 87–94.

James AF, Choisy SC, Hancox JC (2007). Recent advances in understanding sex differences in cardiac repolarization. Prog Biophys Mol Biol 94: 265–319.

Jeong I, Choi BH, Hahn SJ (2011). Rosiglitazone inhibits Kv4.3 potassium channels via open channel block and acceleration of closed-state inactivation. Br J Pharmacol 163: 510–520.

Josephson IR, Sanchez-Chapula J, Brown AM (1984). Early outward current in rat ventricular cells. Circ Res 54: 157–162.

Kilkenny C, Browne W, Cuthill IC, Emerson M, Altman DG (2010). NC3Rs Reporting Guidelines Working Group. Br J Pharmacol 160: 1577–1579.

Kléber AG, Rudy Y (2004). Basic mechanisms of cardiac impulse propagation and associated arrhythmias. Physiol Rev 84: 431–488.

Kneller J, Kalifa J, Zou R, Zaitsev AV, Warren M, Berenfeld O *et al.* (2005). Mechanisms of atrial fibrillation termination by pure sodium channel blockade in an ionically-realistic mathematical model. Circ Res 96: e35–e47.

Kodama I, Kamiya K, Toyama J (1997). Cellular electropharmacology of amiodarone. Cardiovasc Res 35: 13–29.

Lacerda AE, Kuryshev YA, Yan GX, Waldo AL, Brown AM (2010). Vanoxerine: cellular mechanism of a new antiarrhythmic. J Cardiovasc Electrophysiol 21: 301–310.

Mátyus P, Varró A, Papp JG, Wamhoff H, Varga I, Virág L (1997). Antiarrhythmic agents: current status and perspectives. Med Res Rev 17: 427–451.

Makkar RR, Fromm BS, Steinman RT, Meissner MD, Lehmann MH (1993). Female gender as a risk factor for torsades de pointes associated with cardiovascular drugs. JAMA 270: 2590–2597.

Manning AS, Hearse DJ (1984). Reperfusion-induced arrhythmias: mechanisms and prevention. J Mol Cell Cardiol 16: 497–518.

McGrath J, Drummond G, Kilkenny C, Wainwright C (2010). Guidelines for reporting experiments involving animals: the ARRIVE guidelines. Br J Pharmacol 160: 1573–1576.

Nattel S (2002). New ideas about atrial fibrillation 50 years on. Nature 415: 219–226.

Nawrath H (1981). Action potential, membrane currents and force of contraction in mammalian heart muscle fibers treated with quinidine. J Pharmacol Exp Ther 216: 176–182.

Näbauer M, Beuckelmann DJ, Erdmann E (1993). Characteristics of transient outward current in human ventricular myocytes from patients with terminal heart failure. Circ Res 73: 386–394.

Negretti N, O'Neill SC, Eisner DA (1993). The effects of inhibitors of sarcoplasmic reticulum function on the systolic Ca^{2+} transient in rat ventricular myocytes. J Physiol 468: 35–52.

Pogwizd SM, Corr PB (1987). Electrophysiologic mechanisms underlying arrhythmias due to reperfusion of ischemic myocardium. Circulation 76: 404–426.

Sah R, Ramirez RJ, Kaprielian R, Backx PH (2001). Alterations in action potential profile enhance excitation-contraction coupling in rat cardiac myocytes. J Physiol 533: 201–214.

Schlepper M (1989). Cardiodepressive effects of antiarrhythmic drugs. Eur Heart J 10: E73–E80.

Shaw RM, Rudy Y (1997). Electrophysiologic effects of acute myocardial ischemia: a theoretical study of altered cell excitability and action potential duration. Cardiovasc Res 35: 256–272.

Singh BN (1992). Bepridil therapy: guidelines for patient selection and monitoring of therapy. Am J Cardiol 69: 75D–78D.

Singh BN, Nademanee K (1985). Control of cardiac arrhythmia by selective lengthening of repolarization: therapeutic considerations and clinical observations. Am Heart J 109: 421–430.

Slawsky MT, Castle NA (1994). K^+ channel blocking actions of flecainide compared with those of propafenone and quinidine in adult rat ventricular myocytes. J Pharmacol Exp Ther 269: 66–74.

Tahara S, Fukuda K, Kodama H, Kato T, Miyoshi S, Ogawa S (2001). Potassium channel blocker activates extracellular signal regulated kinases through Pyk2 and epidermal growth factor receptor in rat cardiomyocytes. J Am Col Cardiol 38: 1554–1563.

Takács J, Iost N, Lengyel C, Virág L, Nesic M, Varró A *et al.* (2003). Multiple cellular electrophysiological effects of azimilide in canine cardiac preparations. Eur J Pharmacol 470: 163–170.

Talajic M, Papadatos D, Villemaire C, Nayebpour M, Nattel S (1990). Antiarrhythmic actions of diltiazem during experimental atrio-ventricular reentrant tachycardias: importance of use-dependent calcium channel-blocking properties. Circ Res 81: 334–342.

Tsuchihashi K, Curtis MJ (1991). Influence of tedisamil on the initiation and maintenance of ventricular fibrillation: chemical defibrillation by I_{to} blockade? J Cardiovasc Pharmacol 18: 445–456.

Waldo AL, Camm AJ, De Ruyter H, Friedman PL, Macniel DJ, Pauls JF *et al.* (1996). Effect of d-sotalol on mortality in patients with left ventricular dysfunction after recent and remote myocardial infarction. The sword investigators, survival with oral d-sotalol. Lancet 348: 7–12.

Walker MJ, Curtis MJ, Hearse DJ, Campbell RW, Janse MJ, Yellon DM *et al.* (1988). The Lambeth Conventions: guidelines for the study of arrhythmias in ischaemia infarction, and reperfusion. Cardiovasc Res 22: 447–455.

Wijffels MC, Dorland R, Mast F, Allessie MA (2000). Widening of the excitable gap during pharmacological cardioversion of atrial fibrillation in the goat: effects of cibenzoline, hydroquinidine, flecainide, and d-sotalol. Circulation 102: 260–267.

Supporting information

Additional Supporting Information may be found in the online version of this article at the publisher's web-site:

http://dx.doi.org/10.1111/bph.12752

Figure S1 Effects of CIJ-3-2F on LV pressure (LVP) in isolated rat hearts paced at 250 beats per min. (A) Representative continuous recording of LVP showing the concentration-dependent and reversible effect of CIJ-3-2F. (B) Representative tracings of LVP (upper) and dP/dt (lower) on an expanded time scale recorded before, after application and washout of CIJ-3-2F. (C) Mean percent values of LV developed pressure (LVDP), +dP/dt_{max} and –dP/dt_{max} after the application of 3, 10 and 30 μM and after washout of CIJ-3-2F. The predrug values of LVDP, +dP/dt_{max} and –dP/dt_{max} were 20.6 ± 2.6 mmHg, 595 ± 66 mmHg·s^{-1} and 388 ± 53 mmHg·s^{-1} respectively. Data are mean ± SEM from eight preparations. **P < 0.01; significantly different from control.

Figure S2 Effects of DMSO on LV pressure (LVP) in rat isolated hearts paced at 250 beats per min. (A) A representative experiment showing that administration of DMSO vehicle failed to alter LVP in a perfused rat heart. (B) Representative tracings of LVP (upper) and dP/dt (lower) on an expanded time scale recorded before, after application and washout of DMSO. (C) Mean percent values of LV developed pressure (LVDP), +dP/dt_{max} and –dP/dt_{max} after the application of 0.003, 0.01 and 0.03% (v·v^{-1}) and after washout of DMSO. The pre-DMSO values of LVDP, +dP/dt_{max} and –dP/dt_{max} were 28.8 ± 3.0 mmHg, 1012 ± 125 mmHg·s^{-1} and 554 ± 35 mmHg·s^{-1} respectively. Data are mean ± SEM from seven preparations. **P < 0.01, #P < 0.001; significantly different from control.

Figure S3 Effects of DMSO vehicle on Ca^{2+} transients and cell shortening in rat ventricular myocytes. The myocyte was stimulated at 1 Hz. (A,B) Bar graphs showing the averaged data of the effects of DMSO on parameters of $Ca2^{+}$ transients and cell shortening respectively. Cell shortening is normalized to resting cell length. Data are mean ± SEM from 16 experiments.

Figure S4 Concentration-dependent effects of CIJ-3-2F on (A) I_{to} and I_{ss}, (B) I_{Na} and (C) $I_{Ca,L}$ in rat atrial myocytes. The left side of each panel shows the superimposed records of ionic currents in control and in the presence of increasing concentrations of CIJ-3-2F. The right side shows the concentration-response curves obtained with CIJ-3-2F for the inhibition of the integral of I_{to} (n = 8) and the amplitudes of I_{ss} (n = 8), I_{Na} (n = 10) and $I_{Ca,L}$ (n = 8). Continuous lines were drawn according to the fitting of Hill equation. Each data point represents mean ± SEM. The calculated mean IC_{50}, E_{max} and n_H for inhibiting I_{to} integral were 3.9 ± 0.8 μM, 96.2 ± 3.7% and 1.11 ± 0.08 (n = 8); for inhibiting I_{SS} were 1.9 ± 0.5 μM, 61.2 ± 5.4% and 1.17 ± 0.08 (n = 8); for inhibiting I_{Na} were 1.2 ± 0.1 μM, 98.6 ± 1.9% and 1.26 ± 0.09 (n = 10); for inhibiting $I_{Ca,L}$ were 3.4 ± 0.5 μM, 62.3 ± 3.3% and 1.21 ± 0.14 (n = 8) respectively.

Table S1 Effects of increasing concentrations of DMSO on action potentials and contractile forces recorded from rat ventricular papillary muscles and left atrial strips at a stimulation frequency of 1 Hz.